KATHMANDU UNIVERSITY

SCHOOL OF ENGINEERING

DEPARTMENT OF GEOMATICS ENGINEERING

"MACHINE LEARNING & HEC-RAS INTEGRATED MODELS FOR FLOOD INUNDATION MAPPING IN BAGMATI RIVER - KHOKANA, NEPAL"

by

Aasish Shrestha [029036-21]

Arbin Chaudhary [028997-21]

Ganesh Saud [029035-21]

Rajesh Rokaya [028811-21]

Sahadev Sharma [028028-20]

A FINAL YEAR PROJECT REPORT

SUBMITTED TO THE

DEPARTMENT OF GEOMATICS ENGINEERING

IN PARTIAL FULFILLMENT OF THE REQUIREMENTS FOR THE BACHELOR DEGREE IN GEOMATICS ENGINEERING

DEPARTMENT OF GEOMATICS ENGINEERING

DHULIKHEL, KAVRE

FEBRUARY, 2026

CERTIFICATION

This is to certify that the project entitled "**Machine Learning & HEC-RAS Integrated Models for Flood Inundation Mapping in Bagmati River - Khokana, Nepal"** in partial fulfillment of Bachelor Degree in Geomatics Engineering has been evaluated on the basis of their work and oral presentation made by the candidate(s), and found satisfactory.

Date of Evaluation: February 17, 2026

Er. Nisha Adhikari

Chief Survey Officer

Survey Department, Minbhawan Kathmandu

Associate Prof. Dr. Reshma Shrestha

Supervisor

Er. Sujan Subedi

Supervisor

Associate Prof. Dr. Subash Ghimire

Head of the Department

Department of Geomatics Engineering

Kathmandu University

DECLARATION

The authors declare that the complete work presented in this project entitled "**Machine Learning & HEC-RAS Integrated Models for Flood Inundation Mapping in Bagmati River - Khokana, Nepal"** submitted to the Department of Geomatics Engineering at Kathmandu University is our original work performed under the appropriate guidance and supervision of **Dr. Reshma Shrestha and Er. Sujan Subedi**. The authors have likewise consented that the library can make this report openly available for examination. Approval for broad duplication of this report for academic purposes may be given by the supervisor(s) who oversaw the work documented here or, if they are unavailable, by the Head of the Department.

Aasish Shrestha

029036-21

Arbin Chaudhary

028997-21

Ganesh Saud

029035-21

Rajesh Rokaya

028811-21

Sahadev Sharma

028028-20

ABSTRACT

Flooding along the Bagmati River poses a significant threat to communities in the Kathmandu Valley, particularly in Khokana, where rapid urbanization has encroached upon natural floodplains. Traditional hydraulic models often struggle in such environments due to intensive data requirements and a reliance on low-resolution elevation datasets that fail to capture complex micro-topography. To address these limitations, this study integrates an Artificial Neural Network (ANN) with a two-dimensional (2D) HEC-RAS hydraulic model to generate high-accuracy flood inundation maps. The ANN was trained using hydro-meteorological time-series data (rainfall, temperature, and discharge) from 2019 - 2022 and validated against independent 2023 records from the Department of Hydrology and Meteorology (DHM), Nepal. The ANN-predicted discharge served as the upstream boundary condition for the hydraulic simulation, while an ultra-high-resolution (14.9 cm) Digital Terrain Model (DTM) generated via UAV photogrammetry and DGPS surveys ensured explicit representation of embankments and floodplain features.

Model validation was performed by comparing simulated extents with historical flood footprints derived from Landsat imagery using the Normalized Difference Water Index (NDWI). The results indicate that the integrated ANN-HEC-RAS framework provides a robust and reliable alternative to conventional modeling, specifically in capturing the spatial extent of peak flow events. The resulting maps offer a vital tool for local authorities in flood risk assessment, cultural heritage protection, and disaster-resilient urban planning. This research demonstrates a scalable, data-driven approach to flood management in data-scarce and rapidly urbanizing regions, highlighting the potential of combining machine learning with hydraulic modeling to improve resilience against future flood hazards.

Keywords: Artificial Neural Network (ANN); HEC-RAS; Hydrological modeling; NDWI

ACKNOWLEDGEMENT

We would like to express our heartfelt gratitude to everyone who supported us in completing this project, **“MACHINE LEARNING & HEC-RAS INTEGRATED MODELS FOR FLOOD INUNDATION MAPPING IN BAGMATI RIVER - KHOKANA, NEPAL.”**

First of all, we are deeply thankful to our supervisors, **Dr. Reshma Shrestha** and **Er. Sujan Subedi**, for their continuous guidance, encouragement, and insightful feedback throughout the entire process. Their support helped us stay focused and motivated, and their experience was invaluable in shaping the outcome of our study.

We are truly grateful to all the faculty members of the **Department of Geomatics Engineering** for sharing their knowledge, offering helpful feedback, and always being ready to assist us whenever we faced challenges.

A special thank you goes to **Er. Dhirendra Bhatta Deo** from **Amit Consultant Pvt. Ltd.** for kindly providing us UAV (DJI Mavic 2 Pro) battery and for helping us while carrying out UAV Survey. We also appreciate **NEA Engineering Company** Organization for assisting us providing Tribrach for doing DGPS Survey.

We would like to thank the **District Administration Office**, **Lalitpur,** for granting us the necessary permissions and ensuring a smooth and safe drone operation during our data collection phase.

Finally, we express our sincere appreciation to everyone who contributed to this project in any way, from the local communities to technical experts and friends. Your support, directly or indirectly, made this project possible, and we are genuinely thankful for your help.

Thank you all.

Sincerely,

Aasish Shrestha

Arbin Chaudhary

Ganesh Saud

Rajesh Rokaya

Sahadev Sharma

TABLE OF CONTENTS

LIST OF TABLES

LIST OF FIGURES

LIST OF EQUATION

LIST OF ABBREVIATIONS

Abbreviation	Full Form
ANN	Artificial Neural Network
ASTER	Advanced Spaceborne Thermal Emission and Reflection Radiometer
CRED	Centre for Research on the Epidemiology of Disasters
DEM	Digital Elevation Model
DGPS	Differential Global Positioning System
DHM	Department of Hydrology and Meteorology
DTM	Digital Terrain Model
FFA	Flood Frequency Analysis
GCP	Ground Control Point
GIS	Geographic Information System
HEC-RAS	Hydrologic Engineering Center's River Analysis System
ML	Machine Learning
NDWI	Normalized Difference Water Index
NSE	Nash–Sutcliffe Efficiency
RF	Random Forest
R^2	Coefficient of Determination
SRTM	Shuttle Radar Topography Mission
SVM	Support Vector Machine
UAV	Unmanned Aerial Vehicle
USACE	United States Army Corps of Engineers
USGS	United States Geological Survey

CHAPTER ONE: INTRODUCTION

1.1 Background

A flood is a natural phenomenon where an area of land that is usually dry becomes submerged by an overflow of water. In hydrological terms, it occurs when a river's discharge exceeds the capacity of its channel, causing water to spill over its banks onto the surrounding floodplains. Floods can be categorized into various types, such as riverine floods, flash floods, and urban floods, depending on the speed of onset and the landscape (UNESCO, 2023). While flooding is a natural process for river systems, it becomes a disaster when it interferes with human settlements, infrastructure, and the environment.

Flooding is caused by a complex interaction of natural and human-induced factors. Naturally, intense and prolonged rainfall especially during the monsoon season is the primary cause. This is often worsened by the steepness of a watershed, which forces water to flow quickly into river channels. However, human activities have significantly increased flood risks. Rapid urbanization replaces natural soil with impermeable surfaces like concrete and asphalt, preventing rainwater from soaking into the ground and increasing surface runoff. Additionally, deforestation and the encroachment of buildings onto riverbanks reduce the river's natural ability to manage excess water (Thapa et al., 2020).

Studying floods is vital because they are among the deadliest and most expensive natural disasters. For Geomatics engineers, flood studies are important because they allow us to translate complex numerical water data into visual spatial maps. These maps are essential for urban planning, designing resilient infrastructure, and setting up early warning systems that save lives and protect property (Sampson et al., 2015).

On a global scale, floods are the most frequent and costly type of natural disaster. According to the Centre for Research on the Epidemiology of Disasters (Centre for Research on the Epidemiology of Disasters, 2024), floods account for nearly half of all weather-related disasters worldwide. As the global climate changes, extreme weather events have become more unpredictable. Coastal cities face rising sea levels, while inland regions experience "once-in-a-century" floods with increasing frequency. These events result in billions of dollars in economic damage and the displacement of millions of people every year.

Asia is the most flood-prone continent in the world. The region is heavily influenced by the South Asian Monsoon, which brings massive amounts of rainfall in a short period. Large river systems, such as the Ganges, Brahmaputra, and Mekong, support some of the highest population densities on Earth. When these rivers flood, the impact is catastrophic due to the sheer number of people living in low-lying areas (Tamiru & Wagari, 2022a) In many Asian countries, the combination of high-intensity rainfall and unplanned urban growth has made flood management a top priority for national safety.

In Nepal, floods are a recurring annual threat. The country's unique geography dropping from the world's highest mountains to the flat Terai plains in a very short distance creates a high-energy environment for water. During the monsoon (June to September), Nepal receives about 80% of its annual rainfall. This leads to massive riverine flooding and landslides. Historically, events like the 1993 flood in Central Nepal demonstrated the extreme vulnerability of the country, causing massive loss of life and destroying vital infrastructure like bridges and dams (Gautam & Kharbuja, 2006).

The Kathmandu Valley has seen an unprecedented rate of urban expansion over the last few decades. The Bagmati River, the valley's primary watercourse, has suffered from significant encroachment. Its natural floodplains have been filled with houses and roads, leaving no room for the river to expand during heavy rains.

Our study focuses on Khokana, a traditional settlement in the southern part of the valley. Khokana is a critical area because the Bagmati River enters a narrower reach here. During peak monsoon periods, the river discharge often exceeds the channel capacity, leading to inundation of agricultural lands and nearby settlements. Because Khokana is a site of great cultural and historical importance, accurate flood mapping is essential to protect its heritage and the livelihoods of its residents.

Traditional hydrological models often require a vast amount of physical data (like soil type, moisture levels, and detailed vegetation maps), which is hard to find in Nepal. To overcome this, we use Artificial Neural Networks (ANN). ANN is a Machine Learning technique inspired by the way the human brain works. It is excellent at finding patterns in complex data. In this study, we provide the ANN with historical rainfall and temperature data, and it learns to predict the resulting river discharge (runoff). This "data-driven" approach allows for highly accurate predictions even when physical watershed parameters are incomplete (Abhishek et al., 2012).

While ANN tells us how much water is coming, HEC-RAS (Hydrologic Engineering Center's River Analysis System) shows us where that water will go. HEC-RAS is a specialized hydraulic modeling software developed by the U.S. Army Corps of Engineers. It takes the river discharge values and moves them through a digital representation of the river channel. By using a high-resolution Digital Terrain Model (DTM), which we generated using UAV (Drone) photogrammetry and DGPS. HEC-RAS can simulate the depth and spread of water across the landscape with high precision (United States Army Corps of Engineers, 2020).

The integration of these two technologies creates a powerful tool for flood management. The ANN model acts as the "brain" that predicts the volume of water based on weather data. This output is then fed into HEC-RAS, which acts as the "visualizer" to map the exact extent of the flood. This integrated approach reduces the uncertainties found in traditional forecasting. By using our locally collected high-resolution DTM data from UAV surveys, we can produce much more detailed inundation maps than those created using low-resolution satellite data. This allows for better planning and preparedness at the local level in Khokana.

1.2 Statement of Problem

Flooding is a frequent and destructive natural hazard in Nepal, significantly impacting communities along the Bagmati River. Despite these recurrent disasters, the Khokana area lacks detailed, locally validated flood inundation maps. A primary challenge is that most existing models for this region rely on low-resolution global elevation data, which fails to capture the actual topography of riverbanks and floodplains, resulting in inaccurate predictions of water spread during monsoon events.

Furthermore, traditional hydrological models often struggle to capture the complex, non-linear, and "flashy" nature of the Bagmati River. These models typically require extensive, high-quality datasets and intensive calibration that are often unavailable in data-scarce regions. Without a reliable method to link accurate rainfall-runoff predictions with high-resolution terrain data, local authorities and planners face significant barriers to effective disaster preparedness and land-use planning.

1.3 Objectives

The main objective of this study is to simulate flood inundation by integrating a Machine Learning- ANN rainfall-runoff model with HEC-RAS.

The specific sub-objectives are:

1. To generate a high-resolution Digital Terrain Model (DTM) of the Bagmati reach at Khokana using UAV photogrammetry and DGPS-based Ground Control Points (GCPs).
2. To develop a reliable Machine Learning model (ANN) using meteorological and hydrological data to predict river discharge.
3. To develop precise spatial flood inundation maps for the Bagmati River-Khokana area.
4. To validate the model's accuracy using remote sensing indicators, such as the Normalized Difference Water Index (NDWI), and historical flood data.

1.4 Scope of Study

The scope of this study is centered on the southern reach of the Bagmati River in the Khokana area, focusing on the technical integration of geomatics and machine learning tools for flood simulation. The research utilizes a high-resolution Digital Terrain Model (DTM) generated from primary field data collected through UAV photogrammetry and DGPS-based ground control points. Methodologically, the work is limited to the integration of an Artificial Neural Network (ANN) to predict river discharge and HEC-RAS for simulating hydraulic flow across the terrain. The final output is strictly confined to flood inundation mapping, which provides a spatial visualization of the depth and extent of floodwaters. Future work could emphasize integrating climate and hydrological variability, expanding to advanced hydrodynamic simulations, and coupling flood models with socio-economic risk assessments to strengthen disaster preparedness and sustainable land-use planning.

1.5 Outline of the Project

This report is divided into five chapters:

- Chapter One introduces the study, its significance, the problem it addresses, and the specific objectives.
- Chapter Two reviews the existing literature on the Bagmati River, Artificial Neural Networks, and the principles of HEC-RAS modeling.
- Chapter Three describes the detailed methodology, including DGPS/UAV fieldwork, ANN training, and the hydraulic simulation process.
- Chapter Four presents the results, including the high-resolution DTM and the final flood inundation maps.
- Chapter Five concludes the report with a summary of findings and recommendations for future work in local flood management.

CHAPTER TWO: LITERATURE REVIEW

2.1 The Evolution of Flood Modeling Approaches

The scientific approach to flood inundation mapping has traditionally been dominated by process-based (or physically-based) hydraulic models. In these models, with the Hydrologic Engineering Center's River Analysis System (HEC-RAS) being a globally recognized standard, flood dynamics are simulated by numerically solving fundamental equations of fluid mechanics, such as the Saint-Venant equations for one-dimensional flow or the Shallow Water Equations for two-dimensional flow. The primary strength of this approach can be attributed to its ability to provide detailed and physically realistic simulations of flood depth, velocity, and spatial extent. However, the fidelity of these models is intrinsically tied to the quality of their input data. A significant limitation is often encountered with the hydrological boundary conditions that define the volume and timing of water entering the river system (i.e., the flood hydrograph). In many regions, and particularly in developing nations, significant uncertainty is introduced by the scarcity of long-term, river discharge data, which often becomes the weakest link in the modeling chain. To mitigate this critical limitation, a significant paradigm shift is being experienced by the field toward integrated, data-driven modeling frameworks. This evolution is characterized by a move away from a sole reliance on process-based models towards the development of hybrid models. As reviewed by (Sharma & Gupta, 2021), in these hybrid approaches, the predictive power of data-driven techniques, such as Machine Learning (ML), for the hydrological component is combined with the detailed simulation capabilities of physical models for the hydraulic component. Through this integration, the strengths of both paradigms are leveraged: complex systems are modeled from available data by ML, while detailed spatial outputs based on fundamental hydraulic principles are provided by physical models.

2.2 Machine Learning in Hydrological Modeling

A powerful and increasingly robust alternative to traditional rainfall-runoff modeling is offered by Machine Learning. Its core advantage can be attributed to the ability to learn and approximate complex, non-linear relationships directly from historical data (e.g., rainfall, temperature, soil moisture) without requiring explicit, pre-defined physical equations. ML is therefore considered particularly well-suited for hydrological applications where underlying processes are intricate and difficult to parameterize. A wide array of ML algorithms has been successfully applied in hydrology, including Artificial Neural Networks (ANNs), Support Vector Machines (SVMs), Random Forests (RFs), and, more recently, deep learning methods like Long Short-Term Memory (LSTM) networks, which are adept at handling time-series data (Mosavi et al., 2018). A prominent and validated example of this application is found in the study by (Tamiru & Wagari, 2022b) in the Baro River Basin, Ethiopia. In their work, an ANN was successfully employed to predict daily river discharge using readily available meteorological inputs, where it was demonstrated that ML can effectively bridge a critical data gap and generate reliable hydrological boundary conditions. Methodological guidance is also provided by a complementary study by (Wedajo et al., 2024) in the Awash Basin. In their work, the critical importance of using data-driven feature selection techniques to identify the most influential local flood causative factors before model training was emphasized. This is a key best-practice in any ML workflow, as it ensures that the model is trained on the most relevant predictors, thereby improving its accuracy and robustness.

$$\text{Weights} = \begin{bmatrix} w_{11} & w_{12} & w_{13} & w_{14} \\ w_{21} & w_{22} & w_{23} & w_{24} \\ w_{31} & w_{32} & w_{33} & w_{34} \\ w_{41} & w_{42} & w_{43} & w_{44} \end{bmatrix}$$

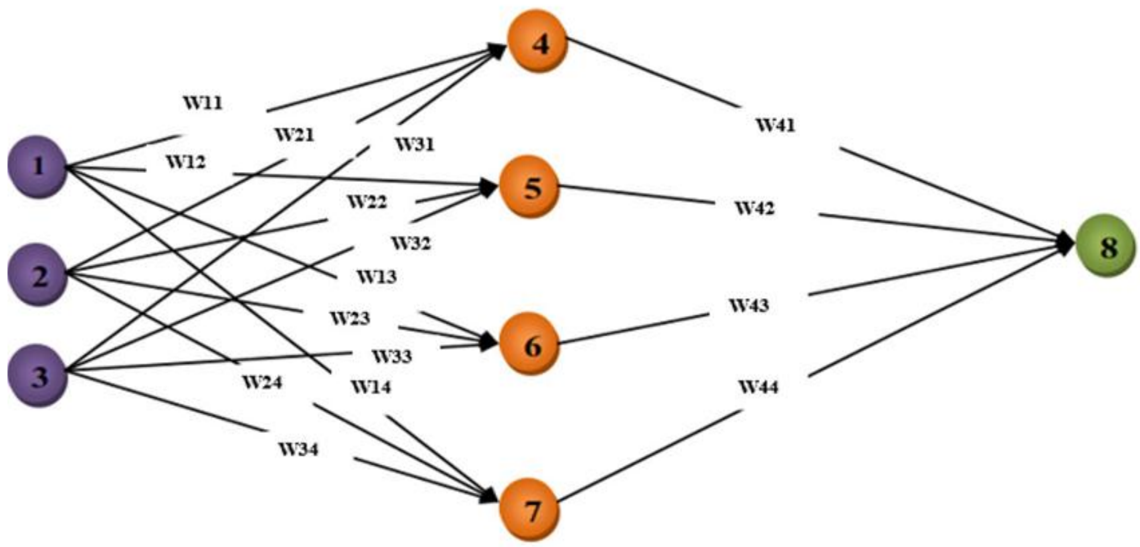

Figure 1: Assigned initial weights in the ANNs

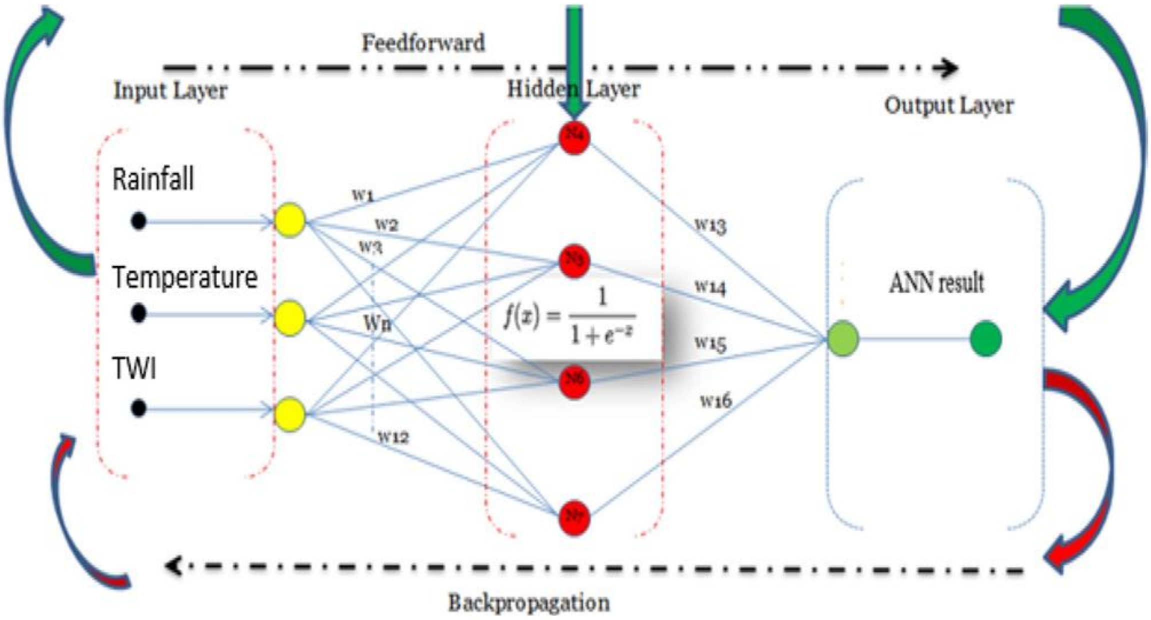

Figure 2: The conceptual ANN architecture for feedforward and back propagation processes

2.3 HEC-RAS in Flood Inundation Mapping

Within the hybrid modeling framework, HEC-RAS is utilized as the hydraulic simulation engine. Its enduring relevance as a cornerstone of detailed flood inundation mapping can be attributed to its robust capacity for both one-dimensional (1D) and two-dimensional (2D) hydraulic simulations. While 1D modeling is computationally efficient for the simulation of flow confined within a well-defined river channel, 2D modeling is considered essential for the accurate simulation of complex overland flow across broad floodplains and within urban or peri-urban environments like Khokana. In such areas, flow paths are not linear and are heavily influenced by structures and micro-topography. The core function of HEC-RAS is characterized by the processing of three primary categories of input to simulate how water moves across the landscape: Geometric Data: The physical shape of the river and floodplain is defined by this data. For 1D modeling, this consists of river cross-sections. For 2D modeling, a computational mesh is built from a high-quality Digital Elevation Model (DEM). Hydraulic Parameters: Surface roughness coefficients (e.g., Manning's 'n' values), which account for friction from different land cover types (e.g., fields, roads, vegetation), are included in this category. Boundary Conditions: The hydrological input, typically a flood hydrograph (flow over time) at the upstream end of the model reach, is provided as the boundary condition. This is the critical point of integration where the output from the ML hydrological model is used as the input for HEC-RAS.

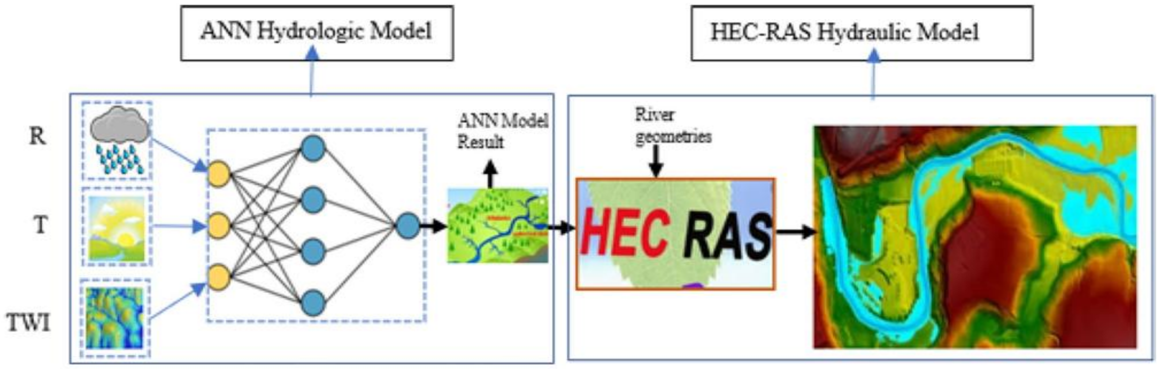

Figure 3: ANN and HEC-RAS integrated conceptual framework

2.4 A Quantitative Framework for Model Performance and Validation

The credibility of any computational model is established through a rigorous and quantitative evaluation of its performance. A clear and comprehensive framework for such validation is provided by the research conducted in Ethiopia. For the hydrological component, a suite of statistical indices is deemed essential. As established by (Tamiru & Wagari, 2022b), a standard validation suite is formed by the Nash-Sutcliffe Efficiency (NSE) (target > 0.75 for "Very good"), Percent Bias (PBIAS) (target < ±10% for "Very good"), and the Coefficient of Determination (R^2) (target ≥ 0.85 for "Very good"). For the final spatial inundation map, a direct measure of accuracy is offered by the Overlapping Percentage Agreement, where a spatial overlap of more than 85% between the simulated and observed flood is considered a "good agreement" (Tamiru & Wagari, 2022b). Adherence to these established metrics is considered critical for ensuring the results of this thesis are comparable and scientifically credible.

$$NSE = 1 - \sum_{i=1}^{n} (Q_O - Q_S)^2 \Big/ \sum_{i=1}^{n} (Q_O - Q_{mean})^2$$

Equation 1: Nash–Sutcliffe model efficiency coefficient (NSE)

Where, Q_O = Observed values

Q_S = Simulated/predicted values

Q_{mean} = Mean of observed values

n = Number of observations

i = Index from 1 to n

$$PBIAS(\%) = \sum_{i=1}^{n} \left(Y_{i(Obs)} - Y_{i(Sim)}\right) * 100 \Big/ \sum_{i=1}^{n} \left(Y_{i(Obs)}\right)$$

Equation 2: Percent Bias

Where,

$Y_{i(Obs)}$ = Array/vector of observed values

$Y_{i(Sim)}$ = Array/vector of simulated values

n = Number of observations

$$NDWI = Green - NIR/Green + NIR$$

Equation 3: Normalized Difference Water Index (NDWI)

Where,

NIR = Near-Infrared band reflectance

2.5 The Role of High-Resolution Topography and UAV DEM

The accuracy of any flood inundation model is fundamentally constrained by the quality of the topographic data used. In most regional flood studies, publicly available, satellite-derived Digital Elevation Models (DEMs) with resolutions of 12.5m to 30m are commonly utilized. While suitable for large basins, this resolution is considered insufficient for the accurate modeling of flood dynamics in complex urban or peri-urban landscapes (Bhattacharya et al., 2020). A transformative technological advancement is represented by the use of Unmanned Aerial Vehicles (UAVs) for topographic surveying. As has been demonstrated in geomatics conferences, UAV-based photogrammetry is now considered a best-practice for the creation of high-fidelity DEMs for local-scale hydraulic studies, through which centimeter-level resolution can be achieved (Horstmann & Wenzel, 2019). Through this method, the explicit representation of critical anthropogenic features that control flood pathways is made possible.

2.6 Flood Studies in Nepal and the Bagmati Basin

Flood research within Nepal, and specifically the Bagmati Basin, has been a sustained area of academic and governmental focus due to the region's high vulnerability to monsoonal flooding, which is exacerbated by rapid urbanization. In previous studies, a predominant reliance was placed on conventional methodologies. Hydraulic modeling using HEC-RAS has been a common approach, often where discharge data from the Department of Hydrology and

Meteorology (DHM) and globally available DEMs like SRTM or ASTER were utilized for inundation mapping (e.g.(Adhikari & Sharma, 2018; Pandey et al., 2020)). While these studies are foundational, limitations related to the sparsity of river gauging stations and the coarse resolution of the topographic data are often acknowledged. Statistical and GIS-based approaches have also been the focus of other research. Flood Frequency Analysis (FFA) using historical peak flow data has been employed to estimate flood return periods (e.g.(Shrestha, 2019)). Additionally, remote sensing and GIS have been used to create broader flood hazard zonation maps based on factors like proximity to rivers, elevation, and land use. While these efforts are crucial for regional planning, the detailed, site-specific inundation information needed for local risk management in densely populated areas like Khokana is typically lacking. Conspicuously absent from the published literature for the Bagmati Basin is the application of integrated, hybrid models where machine learning and detailed hydraulic simulations are coupled, particularly when enhanced with ultra-high-resolution topographic data.

2.7 Research Gap and Conceptual Framework

As demonstrated by this review, the literature provides a validated pathway for advanced flood inundation mapping through the integration of machine learning with HEC-RAS. However, a significant research gap remains in applying this integrated methodology within fundamentally different environmental and geographical contexts. This gap can be understood in two distinct dimensions:

A Contextual Gap: This gap is characterized by the unique characteristics of the study area. The referenced benchmark studies were conducted in large, predominantly rural African river basins. In contrast, Khokana, situated within the Bagmati Basin, is a densely populated, peri-urban landscape where rapid and often unplanned urbanization is occurring. Here, flood dynamics are not solely governed by natural rainfall-runoff processes but are heavily influenced by anthropogenic pressures. These include river channel encroachment, the construction of roads and embankments that alter natural drainage paths, and a high percentage of impervious surfaces that accelerate runoff. The performance and adaptability of the integrated ML-HE-RAS model in such a human-modified landscape, where the built environment is a dominant hydraulic control, remains an open and critical question. This gap will be addressed by this thesis through the specific testing of the model's applicability in a context where human factors are as important as natural ones.

A Technological Gap: This gap is related to the limitations of the data used in previous studies. The Ethiopian research, while methodologically sound, was reliant on satellite-derived DEMs with resolutions in the range of meters (12.5m to 30m). Due to this technological constraint, fine-scale features critical in a peri-urban setting could not be 'seen' by their models. This gap will be bridged by this thesis through the incorporation of an ultra-high-resolution DEM derived from a UAV survey. This leap in data quality from meter-level to centimeter-level resolution is not merely an incremental improvement; it is a transformative step by which the explicit representation of features like irrigation canals, road crowns, and small retaining walls within the hydraulic model is allowed. The degree of accuracy improvement that is brought to the integrated modeling framework by this advanced technology will be assessed as a key contribution of this research.

This project will therefore address this dual gap by creating a high-fidelity flood inundation map for a complex, peri-urban environment using an integrated model enhanced with UAV-derived data.

CHAPTER THREE: RESEARCH METHODOLOGY

3.1 Study Area

The study area is situated in the Khokana region of the Bagmati River Basin in central Nepal, extending approximately from 27°37′00″ N to 27°38′15″ N latitude and 85°17′30″ E to 85°18′00″ E longitude. It covers an area of about 1.48 km² with an approximate perimeter of 5.49 km. Administratively, the area falls within Wards 1, 2, and 4 of Dakshinkali Municipality and Wards 21 and 22 of Lalitpur Sub-Metropolitan City, spanning parts of Kathmandu and Lalitpur districts. The landscape is characterized by gently sloping terrain and flat, fertile deposited plains formed by the Bagmati River over time. A large portion of the area consists of low-lying floodplain zones, which makes it particularly vulnerable to seasonal flooding, a key concern addressed in this study.

The Bagmati River is the main geographical feature shaping the study area. It originates in the Shivapuri hills and flows southward through the site, influencing its physical and environmental conditions. A government-operated hydrological gauging station, Khokana Station (No. 550.05), maintained by Nepal's Department of Hydrology and Meteorology (DHM), is located within the study area and provides the river discharge data used in this research.

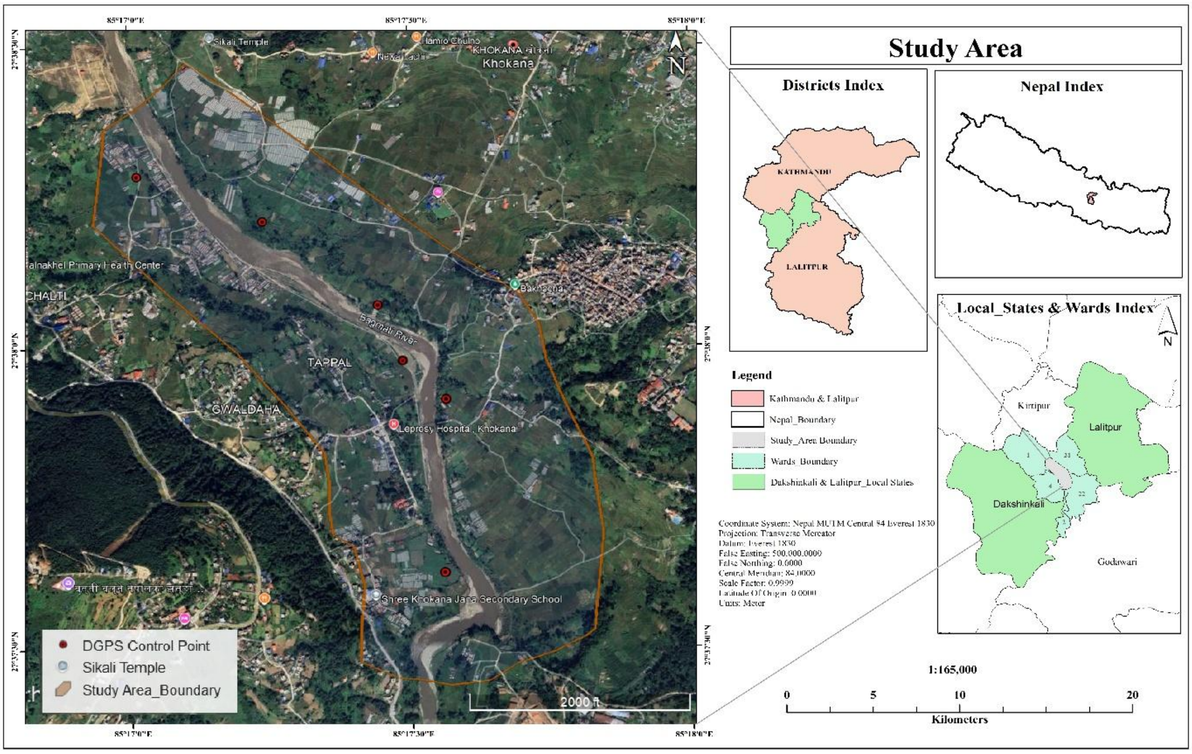

Figure 4: Study Area Map

3.2 Datasets and Software Used

The successful execution of this research relied on a variety of specific datasets, field instruments, and specialized softwares. This section provides a comprehensive summary of the primary and secondary data sources, instruments, and software tools employed throughout the study, from initial data acquisition and processing to modeling, simulation, and final validation. A detailed description of each component's role is presented in below tables.

Table 1: Summary of Datasets and Field Instruments Used

Category	Data/Tool	Sources/Provider	Date/Date Range	Resolution /Interval	Remarks
River Discharge	DHM, Nepal (Khokana Station)	DHM, Nepal	2019-01-01 to 2023-12-31	Daily	Training and testing the ANN hydrological model
Secondary Data	Precipitation (Rainfall, Temperature)	DHM, Nepal	2019-01-01 to 2023-12-31	Daily	Input variables for the ANN hydrological model
Primary Data	Digital Elevation Model (DTM)	UAV Survey Processing	12/27/2025	14.9 cm x 14.9 cm	Primary topographic input for HEC-RAS 2D model
Secondary Data	Landsat 8 Imagery	USGS Earth Explorer	8/8/2023	30 m	Delineation of historical flood extent using NDWI for HEC-RAS validation
Field Instruments	UAV System (DJI Mavic 2 Pro)	-	-	-	Capturing high resolution aerial photographs over the study area
Field Instruments	GNSS Receiver (Spectra Precision SP60)	-	-	-	Establishing high-accuracy Ground Control Points (GCPs)

Table 2: Summary of Software Tools Used in the Study

Category	Software/ Application	Remarks
UAV Data Processing	Pix4Dmapper	Processing raw UAV imagery into georeferenced DTM and Orthomosaic
GIS & Spatial Analysis	ArcGIS 10.8	Spatial data management, HEC-RAS input preparation, and result visualization
Hydrological Modeling	Visual Studio Code (with Python)	Development, training, and testing of ANN model
Hydraulic Simulation	HEC-RAS (6.7)	Execution of 2D unsteady flow hydraulic model for flood inundation simulation
Cloud GIS Platform	Google Earth Engine	Processing satellite imagery and calculating NDWI for validation
Data Management	Microsoft Excel	Organization, pre-processing, and analysis of DHM time-series data
UAV Flight Planning & Survey Software	DroneDeploy	Used for automated flight planning, mission control, and systematic aerial image acquisition for mapping surveys
UAV Control & Monitoring Application	DJI Go 4	Used for manual drone control, camera operation, and real-time monitoring during UAV data capture

3.3 Methodology

In this research, UAV-derived primary data, including the Digital Terrain Model (DTM), were collected, alongside secondary data from DHM, such as river discharge and precipitation. These datasets were carefully processed and employed to develop an Artificial Neural Network (ANN) model for predicting river discharge. The discharge predicted by the ANN model was then used as a boundary condition in the HEC-RAS 2D hydraulic model to simulate flood inundation. Finally, the simulated flood extents were validated by comparison with historical flood observations derived from Landsat imagery and NDWI analysis, ensuring the reliability of the modeling approach.

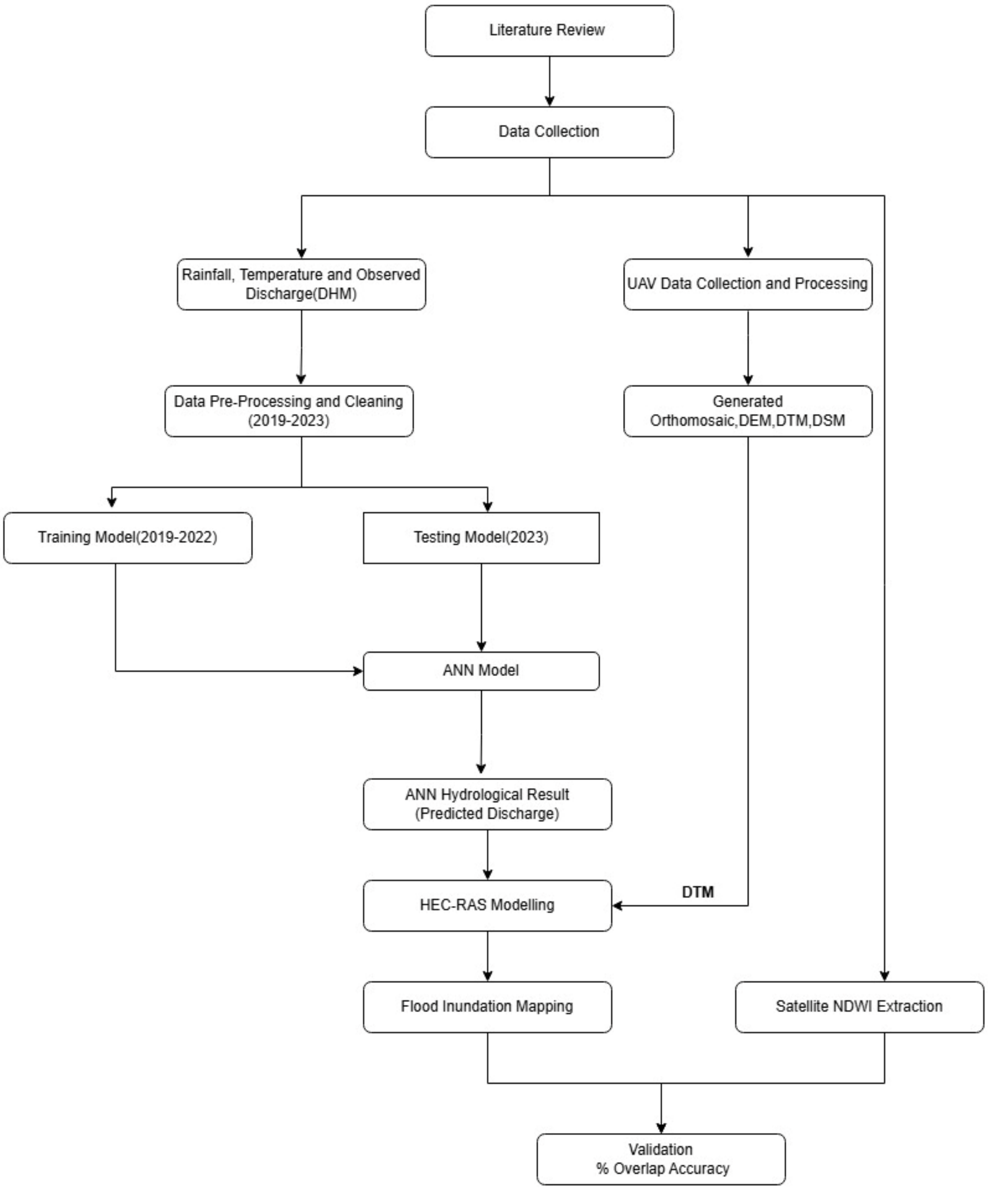

Figure 5: Workflow

3.3.1 Data Collection

The data collection phase was structured into two primary components: hydro-meteorological time-series data used for hydrological modeling and high-resolution topographic data obtained for hydraulic simulation.

Hydro-Meteorological Data

For the development and calibration of the Artificial Neural Network (ANN) model, five years of daily hydro-meteorological data (January 2019 to December 2023) were acquired from the Department of Hydrology and Meteorology (DHM), Nepal. The chosen study period captures recent hydrological behavior and significant weather events in the Khokana region.

Daily river discharge (Q) records were obtained exclusively from the **Khokana Gauging Station (Station No. 550.05),** which is located within the study area and served as the sole hydrological reference point for this research. The raw discharge records were compiled into a continuous daily time series to provide a reliable target dataset for model development. The following figures shows the daily Discharge sample given by this station.

Daily rainfall and temperature records were collected from a network of a 7 surrounding meteorological stations in order to capture the spatial variability of climatic conditions within the catchment area.

Table 3: Rainfall and Temperature Station in the study area

Station Index	Name	District	Latitude (deg)	Longitude (deg)	Elevation (m)
1029	Khumaltar	Lalitpur	27.651677	85.325693	1334
1060	Chapa Gaun	Lalitpur	27.60325833	85.32656389	1478
1073	Khokana	Lalitpur	27.64377222	85.29671667	1309
1075	Lele	Lalitpur	27.57777778	85.35305556	1590
1076	Naikap	Kathmandu	27.70094167	85.255475	1477
1080	Tikathali	Lalitpur	27.659325	85.36970833	1305
1030	Kathmandu Airport	Kathmandu	27.703825	85.35624722	1337

The raw meteorological datasets were filtered and cleaned using Microsoft Excel to identify and correct missing values. After cleaning, the daily rainfall and temperature from all stations were averaged to produce a single representative value for each day of the study period. The processed hydro-meteorological dataset was exported in CSV format and imported into a Python-based modeling environment using Visual Studio Code. Within this environment, the data were normalized and divided into training and testing subsets. The prepared dataset was then employed as the primary input for the ANN framework, allowing the rainfall-runoff relationships to be modeled and river discharge predictions to be generated. The below given table shown the format of csv file imported into the ANN model.

Table 4: Processed hydro-meteorological dataset Sample format

Date	Average_Rainfall (mm)	Average_min_temp (0C)	Average_max_temp (0C)	Discharge (m3/s)	lagged_discharge (m3/s)
1/1/2019	0	0.2	19.1	1.67	0
1/2/2019	0	0.233	18.6	1.69	1.67
1/3/2019	0	-0.2	17.333	4.42	1.69
1/4/2019	0	-0.233	17.133	1.45	4.42
1/5/2019	0	0.567	17.333	1.57	1.45
1/6/2019	0	0.567	19.333	1.3	1.57
1/7/2019	0.3	4.033	15.6	1.36	1.3
1/8/2019	0.257	1.2	19.333	1.32	1.36
1/9/2019	0	2.9	18.7	1.57	1.32
1/10/2019	0	1.8	17.767	1.34	1.57
1/11/2019	0	3.5	17.8	1.4	1.34
1/12/2019	0	3.067	17.567	1.3	1.4
1/13/2019	0	1.7	19.267	0.994	1.3
1/14/2019	0	1.233	18.433	1.16	0.994
1/15/2019	0	0.633	18.5	1.53	1.16
1/16/2019	0	1.533	17.633	1.62	1.53
1/17/2019	0	1.867	18.633	1.57	1.62
1/18/2019	0.314	2	19.567	1.43	1.57
1/19/2019	0.143	2.2	18.6	1.81	1.43
1/20/2019	0	1.933	19.7	1.76	1.81
1/21/2019	0.286	2.667	20.6	1.6	1.76
1/22/2019	0.357	4.2	19.833	1.81	1.6
1/23/2019	11.386	6.767	11.467	1.81	1.81
1/24/2019	3.457	4.867	19.033	2.02	1.81
1/25/2019	1.771	4.667	17.967	2.29	2.02
1/26/2019	6.414	7	13.233	2.31	2.29
1/27/2019	2.971	5.667	17.9	2.13	2.31
1/28/2019	0.086	2.5	17.967	2.02	2.13
1/29/2019	0	2.033	16.9	2.02	2.02
1/30/2019	3.943	0.533	17.933	2.02	2.02
1/31/2019	1.743	2.167	18.5	2.13	2.02
2/1/2019	0	6.2	19.367	2.29	2.13
2/2/2019	0	2.533	20.467	2.02	2.29
2/3/2019	0	1.9	20.9	2.02	2.02
2/4/2019	0	2.667	21.333	1.81	2.02
2/5/2019	0	3.667	20.533	2.13	1.81
2/6/2019	0.643	4.733	21.333	2.18	2.13
2/7/2019	5.314	7	14.467	2.07	2.18
2/8/2019	15.886	8.433	17.067	3.01	2.07
2/9/2019	17.971	5.5	13.867	27.7	3.01
8/1/2023	10.614	21.467	30.8	94.5	25.4
8/2/2023	14.559	21.167	30.367	43.2	94.5
8/3/2023	1.501	21.867	29.433	25.1	43.2
8/4/2023	0.501	21.133	29.133	20.2	25.1
8/5/2023	1.446	20.433	29.433	17.5	20.2
8/6/2023	12.186	20.567	26.7	41.1	17.5
8/7/2023	16.486	20.533	27.033	33	41.1
8/8/2023	35.714	20.333	26.567	389	33
8/9/2023	15.971	21.067	28.133	38.9	389
8/10/2023	9.986	20.967	29.533	31.8	38.9
8/11/2023	2.1	21.767	29.867	26.9	31.8
8/12/2023	17.871	21.567	27.167	118	26.9
8/13/2023	23.771	20.633	22.633	164	118
8/14/2023	28.529	19.3	24.967	36	164
8/15/2023	0.003	19.3	29.8	27.1	36
8/16/2023	0.001	20.6	28.9	27.5	27.1
8/17/2023	2.073	21.033	30.3	27.3	27.5
8/18/2023	1.346	20.3	30.6	24.9	27.3
8/19/2023	2.9	21.567	30.467	21.8	24.9
8/20/2023	0.529	21.1	30.2	17.6	21.8
8/21/2023	17.8	20.7	24.6	27.5	17.6
8/22/2023	16.757	19.367	28.167	27.1	27.5
8/23/2023	12.043	20.133	25.367	61.7	27.1
8/24/2023	20.871	20.2	27.833	155	61.7
8/25/2023	17.657	20.367	26.933	179	155
8/26/2023	19.443	20.1	27.4	84.8	179
8/27/2023	1.314	20.333	29.1	38.5	84.8
8/28/2023	0	18.833	29.767	38.5	38.5
8/29/2023	0.001	20.467	29.4	34.5	38.5
8/30/2023	0.214	19.933	30.133	27.5	34.5
8/31/2023	0.143	20.5	29.1	26.1	27.5
9/1/2023	0.171	20.033	30.033	27.1	26.1

UAV-DGPS Survey and Topographic Processing

Aerial imagery was captured using DJI UAV platforms (DJI Mavic 2 pro), with flight operations planned and executed through the DroneDeploy and DJI GO 4 applications to ensure systematic coverage of the study area. Flight parameters were optimized to ensure high image overlap, with frontal and side overlaps maintained at 75% and 65%, respectively, to facilitate accurate photogrammetric processing. The following figures present the flight planning in the study area, including all required system settings and configurations.

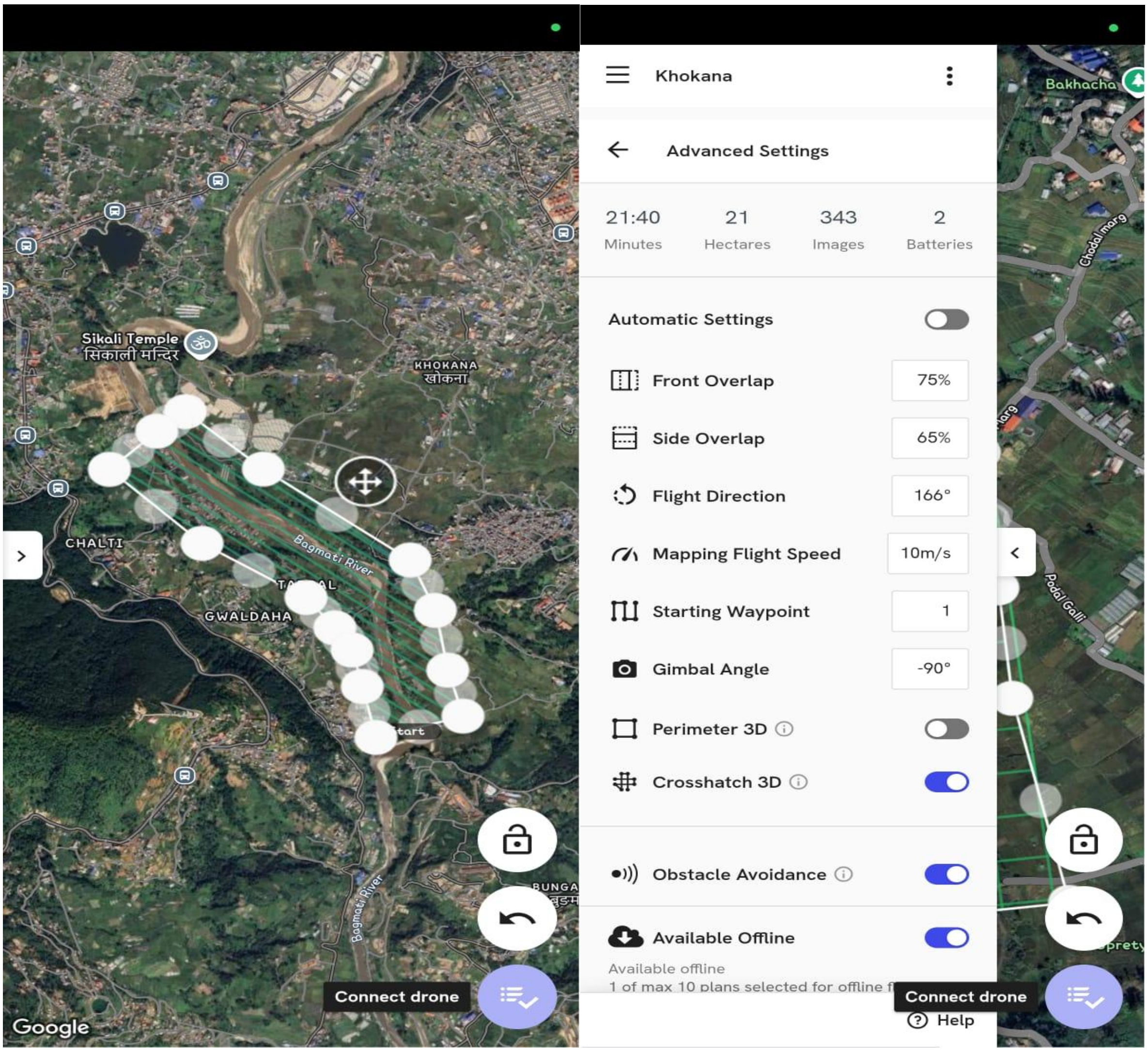

Figure 6: UAV Flight Mission Planning and Optimized Photogrammetric Parameters

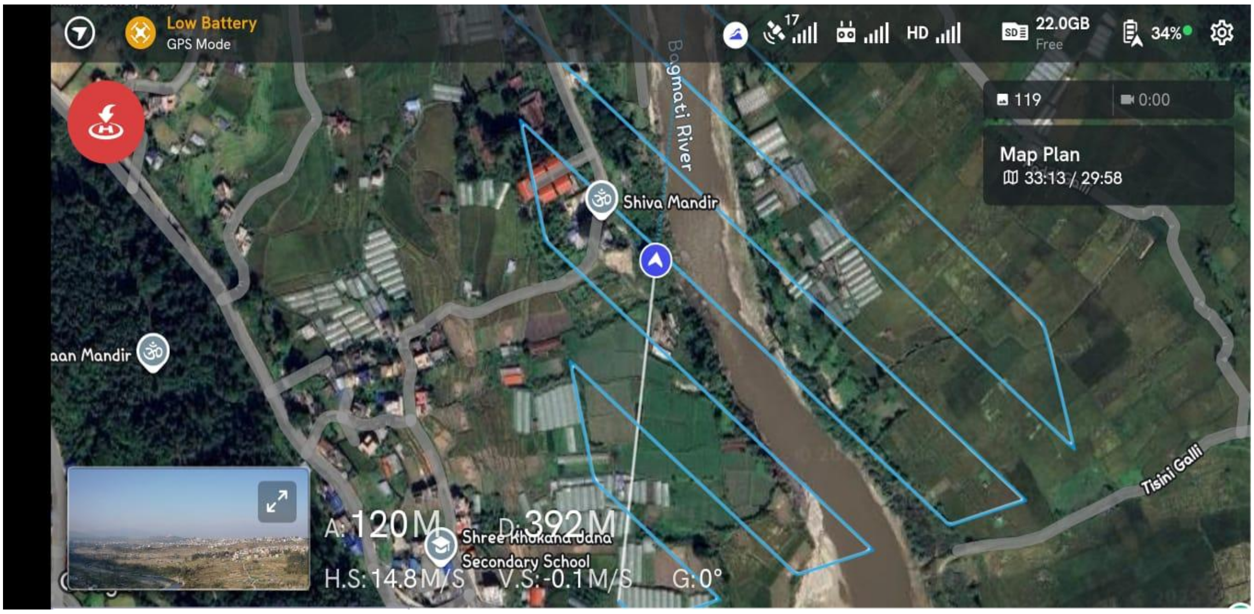

Figure 7: Real-time Flight Monitoring Interface

Prior to the UAV survey, a network of Ground Control Points (GCPs) was established across the study area using a Differential Global Positioning System (DGPS). The base station coordinate was determined through the online processing software AUSPOS and remaining station were calculated using Trimble Business Center (TBC) on the basis of this known base station. These GCPs provided high-precision coordinates (X, Y, and Z-elevation) and were subsequently employed to georeferenced the UAV imagery, minimizing vertical errors and ensuring accurate spatial representation. The following table presents the Ground Control Points (GCPs) established within the study area.

Table 5: DGPS Surveyed Ground Control Points (GCPs)

Name	**Easting (m)**	**Northing (m)**	**Elevation (m)**
khokan5	331391.435	3058008.303	1204.676
khokana1	331492.185	3057787.084	1202.89
khokana2	330652.726	3058411.666	1209.437
khokana3	331617.094	3057139.348	1209.116
Khokana4	331058.168	3058251.303	1213.195
Khokana-base	331619.669	3057669.883	1207.626

The UAV imagery was processed using Pix4Dmapper, employing Structure-from-Motion (SfM) algorithms to generate a dense 3D point cloud of the study area. From this dataset, three primary geospatial products were derived an Orthomosaic, which provided a high-resolution georeferenced base for land-cover mapping and Digital Surface Model (DSM), representing the elevations of all surface features, a Digital Terrain Model (DTM). The DTM provided a 'bare-earth' elevation profile, serving as the fundamental geometric input for the hydraulic simulations. By integrating this high-resolution DTM into HEC-RAS 6.7, the model was able to capture intricate floodplain features, enabling an accurate 2D unsteady flow simulation of the Bagmati River in the Khokana region of Nepal. The generation of the Digital Surface Model (DSM), Orthomosaic, and Digital Terrain Model (DTM) from UAV imagery is illustrated in the figures below. Among these products, the DTM was used as the primary topographic dataset for hydraulic simulation in HEC-RAS.

The accuracy of the georeferenced Orthomosaic was verified by comparing check points to evaluate positional errors. This ensures reliable data for hydraulic modeling and flood inundation analysis.

Table 6: Quality Control Report

Min Error [m]	**Max Error [m]**	**Geolocation Error X [%]**	**Geolocation Error Y [%]**	**Geolocation Error Z [%]**
-	-8.49	0.00	0.00	0.00
-8.49	-6.79	0.00	0.00	0.00
-6.79	-5.10	0.00	0.00	0.00
-5.10	-3.40	0.19	0.28	0.00
-3.40	-1.70	0.33	3.45	0.00
-1.70	0.00	46.78	48.42	41.85
0.00	1.70	51.12	45.90	46.09
1.70	3.40	1.58	0.51	0.00
3.40	5.10	0.00	1.44	0.00
5.10	6.79	0.00	0.00	0.05
6.79	8.49	0.00	0.00	0.09
8.49	-	0.00	0.00	0.00
Mean [m]		0.067636	-0.053239	1.526097
Sigma [m]		0.438793	0.762719	1.127607
RMS Error [m]		0.443975	0.764575	1.400694

Over 97% of geolocation errors in the X and Y directions fall within the range of ±1.7 meters, indicating high horizontal accuracy. The vertical (Z-axis) accuracy, while slightly more variable, remains within ±1.7 meters for nearly 88% of the dataset.

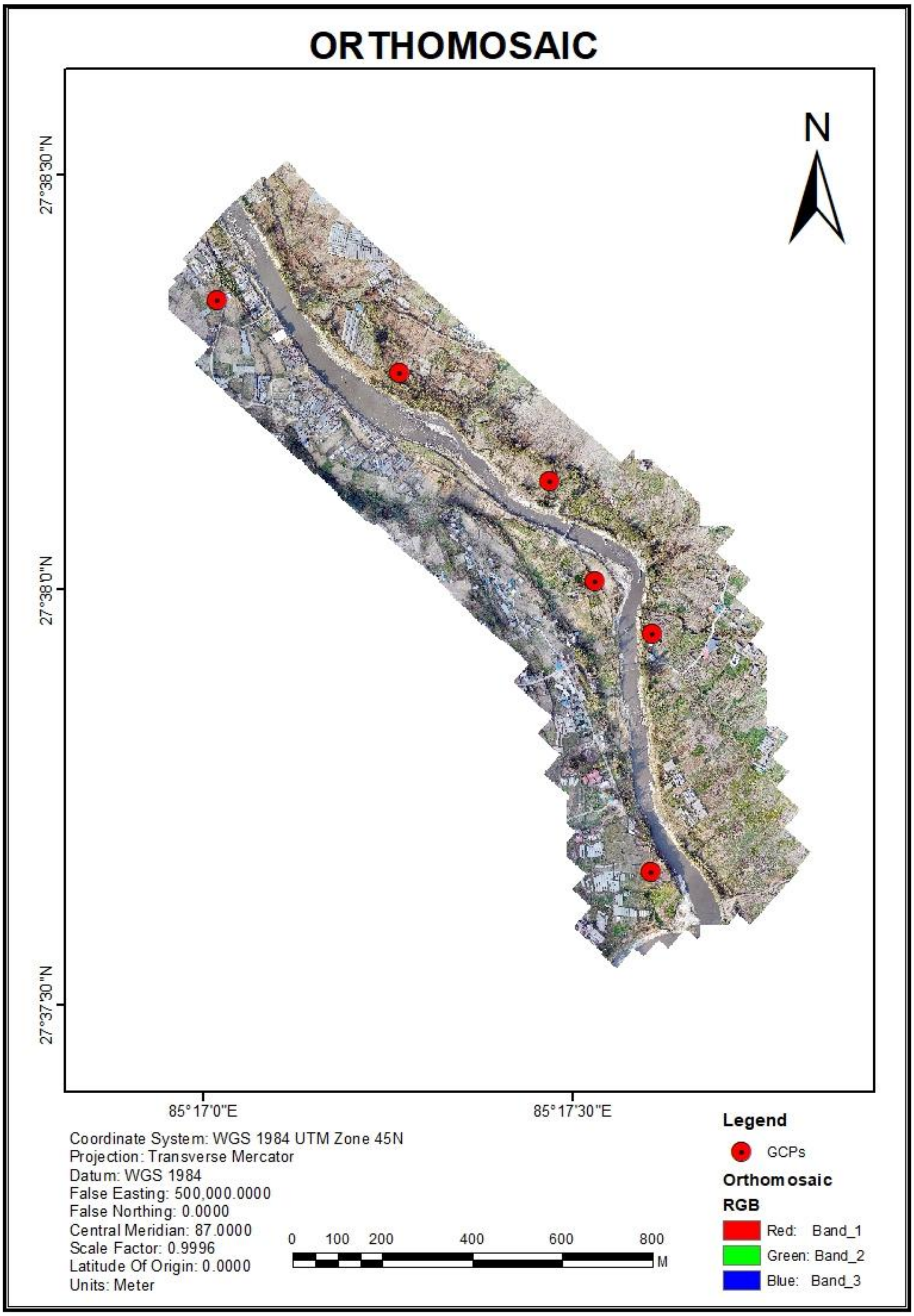

Figure 8: Orthomosaic

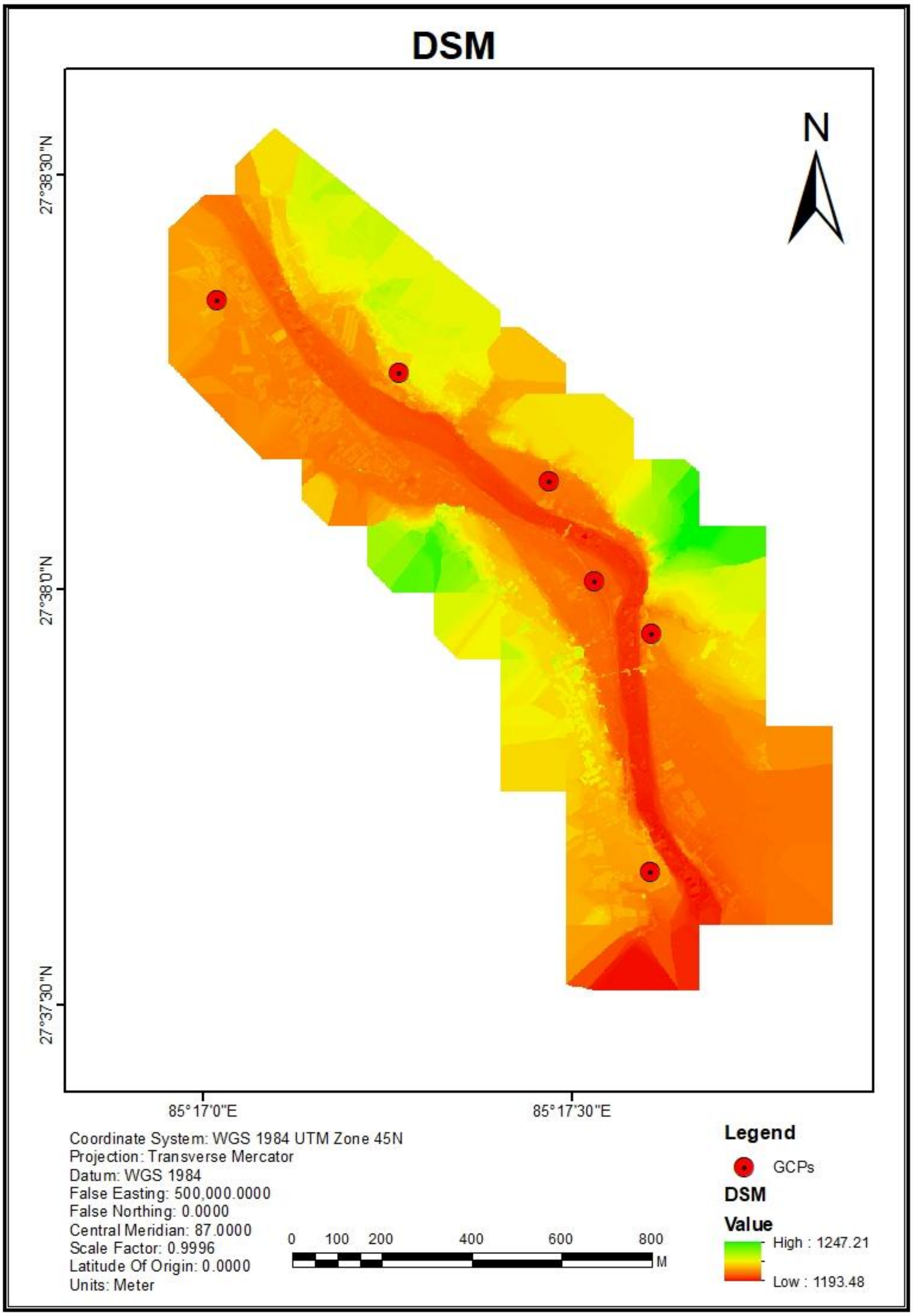

Figure 9: DSM (Digital Surface Model)

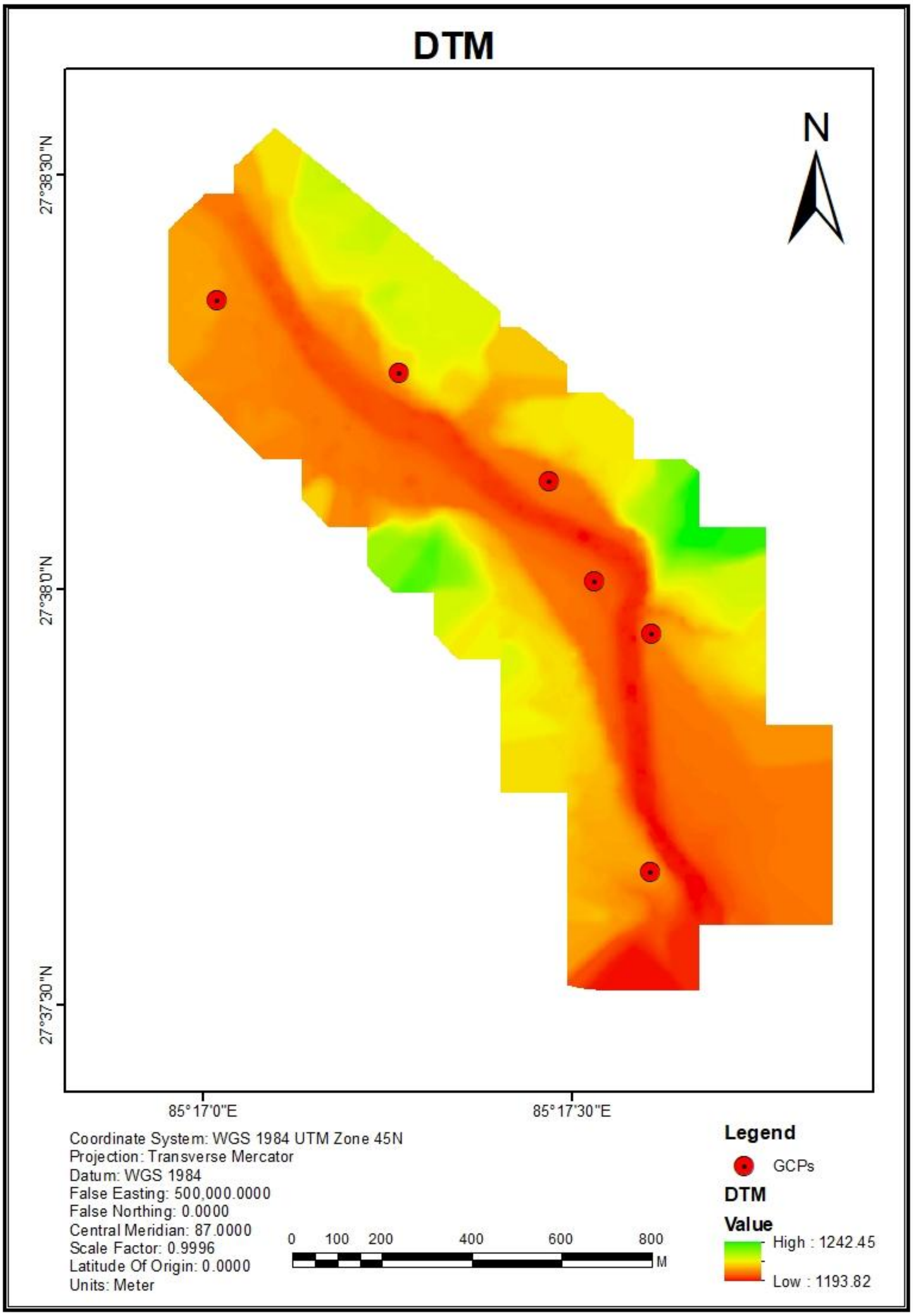

Figure 10: Digital Terrain Model (DTM)

3.3.2 Hydrologic modelling using ANN

In this study, hydrologic runoff generation was modeled using an Artificial Neural Network (ANN), which is a data-driven empirical modeling approach. Unlike physically based hydrologic models, ANN relies on historical relationships between hydro-meteorological variables without explicitly incorporating catchment physical characteristics. The model utilizes ground-based observations such as rainfall, temperature, and gauged discharge to simulate runoff processes. The selected input parameters include: Rainfall (R), Temperature (T), Observed Discharge (Q). The target output of the model is simulated runoff/discharge.

ANN Architecture Design

A feedforward multilayer perceptron (MLP) network with backpropagation learning was employed for runoff prediction. The network architecture was selected based on the number of input/output variables It consists of an input layer with 4 nodes (R, T_{max}, T_{min} Q), a hidden layer with 4 nodes, and an output layer with 1 node (simulated runoff). This 4-4-1 configuration effectively balances network complexity and generalization capability.

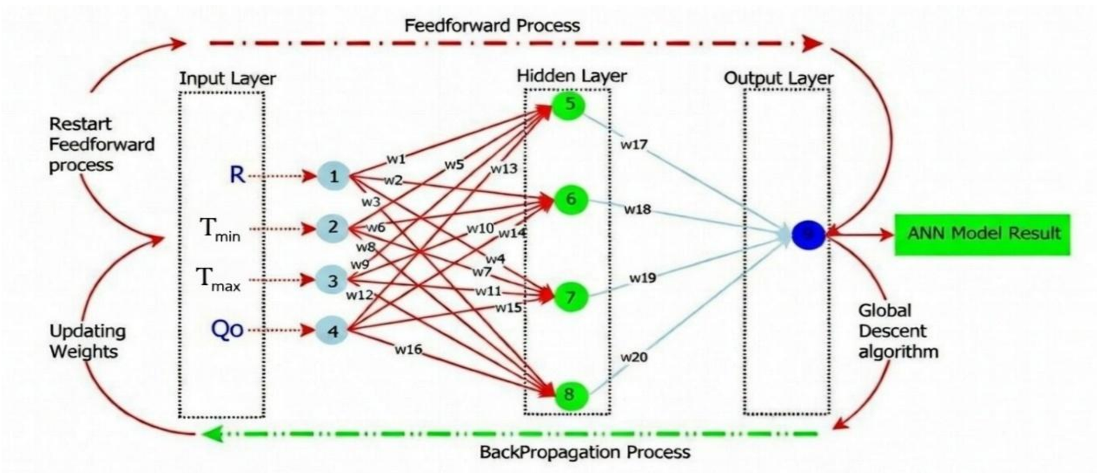

Figure 11: The conceptual ANN architecture for Feedforward and Back propagation Processes

Network Initialization

Synaptic weights between the input-hidden and hidden-output nodes were randomly initialized to break symmetry and enable the network to learn effectively. Each hidden and output node included a bias term to enhance model flexibility.

Activation Function

Rectified Linear Unit activation functions were applied in all hidden layers to introduce nonlinearity and improve gradient propagation in the deep network. For the output layer, a linear activation function was applied to allow for continuous output values suitable for runoff prediction.

$$Activation\ Function = \ 1/1 + e^{x}$$

Equation 4: Activation function

Feedforward Computation

During feedforward propagation, each hidden node receives inputs from all input nodes, which are multiplied by their corresponding weights to compute a weighted sum. These weighted sums are then passed through the sigmoid activation function to introduce nonlinearity. The outputs from the hidden nodes are subsequently multiplied by the weights connecting to the output node, summed, and passed through the linear activation function to generate the simulated discharge.

ANN Training Using Backpropagation

The network was trained using the backpropagation algorithm with gradient descent optimization, which iteratively updates the weights to minimize the error between the simulated and observed discharge values. This learning process allows the network to capture complex, nonlinear relationships between rainfall, temperature, and discharge.

Training Steps

The training process involves several iterative steps. First, forward propagation is performed, where input data is fed through the network to produce an initial output. Next, the error is calculated as the difference between the observed and simulated discharge. Then, backpropagation occurs, propagating the error backward through the network and adjusting the weights using gradient descent. These steps are repeated until convergence criteria are met, such as reaching a predefined error threshold or completing a maximum number of epochs.

Integration of ANN with HEC-RAS

To generate flood inundation maps, the trained ANN runoff outputs were coupled with HEC-RAS hydraulic modeling software. ANN receives daily rainfall and temperature inputs to compute runoff. Simulated runoff values are exported as upstream boundary input to HEC-RAS. HEC-RAS simulates river hydraulics and flood propagation based on channel geometry, flow, and boundary conditions. Spatial flood extent is generated for each simulation period.

This integration enables hydrologic–hydraulic modeling, providing a seamless connection between rainfall–runoff modeling and flood mapping. This learning process allows the network to learn complex, nonlinear relationships between rainfall, temperature, and discharge.

HEC-RAS Model Setup for Flood Inundation Mapping

Hydraulic flood inundation modeling in this study was performed using HEC-RAS Version 6.7, developed by the U.S. Army Corps of Engineers. A two-dimensional (2D) unsteady flow simulation approach was adopted to accurately represent the spatial and temporal dynamics of flood propagation across the floodplain.

Terrain Data Preparation

The first step in hydraulic model development involved the preparation and integration of terrain data. A high-resolution Digital Terrain Model (DTM) of the study area was imported into the HEC-RAS RAS Mapper environment to serve as the base terrain for hydraulic computations. The terrain model was processed to ensure proper vertical datum consistent, and adequate spatial resolution for floodplain representation. This terrain surface formed the foundation for defining flow areas, elevations, and hydraulic connectivity within the 2D domain.

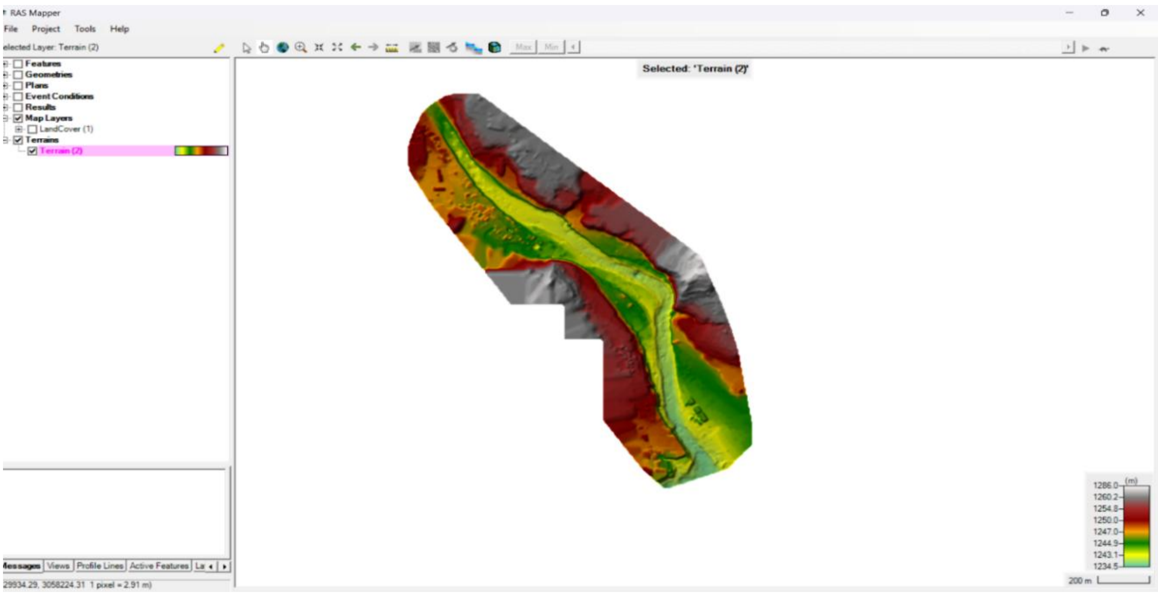

Figure 12: DTM imported in HEC-RAS

Creation of 2D Flow Area

A 2D Flow Area was delineated covering the river channel and adjacent floodplain likely to be affected during high-flow events. The boundary of the 2D domain was digitized within RAS Mapper based on topography and river morphology. Within the 2D flow area, computational cells were generated automatically and cell size was selected to balance computational efficiency and spatial accuracy. The resulting computational mesh allowed simulation of lateral water movement and storage across the floodplain.

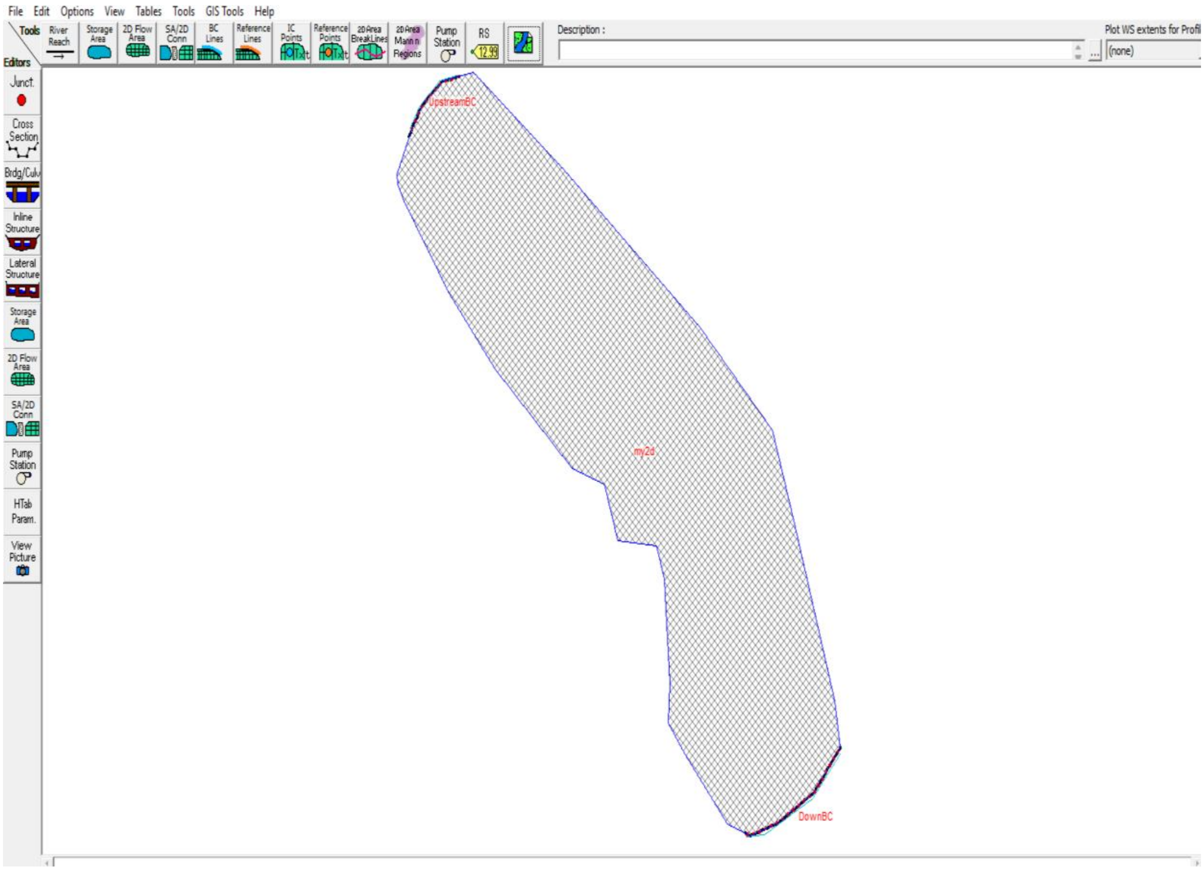

Figure 13: 2D Flow Area

Hydraulic Geometry and Parameterization

Hydraulic properties required for 2D simulation were assigned as follows. Manning's roughness coefficients (n values) were specified based on land use/land cover characteristics such as river channel, vegetation, agricultural land, and built-up areas. Terrain elevations governed flow direction and depth calculations within each computational cell.

	ID	Name	ManningsN	Percent Impervious	Spiral Intensity Source
	0	NoData			
	1	River	0.03		
	2	Forest	0.05		
	3	Grass	0.03		
	4	Flooded Vegetation	0.045		
	5	Cropland	0.025		
	6	Shrubs	0.035		
	7	Buildup	0.013		
	8	Baresoil	0.025		

Figure 14: Mannings Coefficient

Unsteady Flow Data Setup

An unsteady flow simulation was configured to capture the temporal variation of discharge during flood events. Key components included a simulation time window corresponding to the selected flood event, a computational time step suitable for numerical stability, and output intervals for water surface and depth mapping.

Boundary Condition: Flow Hydrograph

The upstream boundary condition was defined using a flow hydrograph representing peak discharge conditions. In this study, a specific high-discharge day was selected based on ANN-predicted runoff records for 2019 and 2023, and the discharge hydrograph corresponding to this event was input at the upstream boundary of the 2D flow area. This hydrograph served as the driving force for flood wave propagation. Downstream boundary conditions were defined using normal depth or stage conditions based on channel slope and available data.

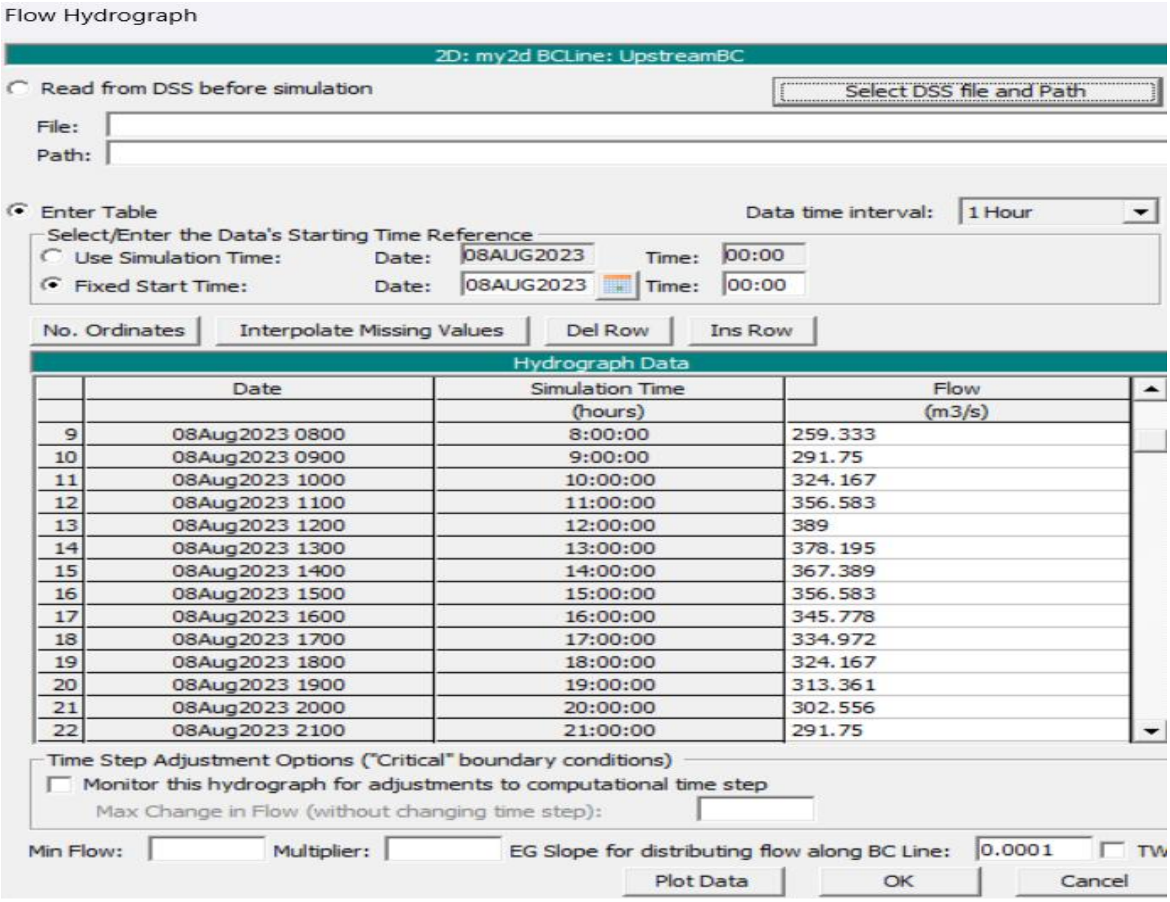

	Date	Simulation Time (hours)	Flow (m3/s)
9	08Aug2023 0800	8:00:00	259.333
10	08Aug2023 0900	9:00:00	291.75
11	08Aug2023 1000	10:00:00	324.167
12	08Aug2023 1100	11:00:00	356.583
13	08Aug2023 1200	12:00:00	389
14	08Aug2023 1300	13:00:00	378.195
15	08Aug2023 1400	14:00:00	367.389
16	08Aug2023 1500	15:00:00	356.583
17	08Aug2023 1600	16:00:00	345.778
18	08Aug2023 1700	17:00:00	334.972
19	08Aug2023 1800	18:00:00	324.167
20	08Aug2023 1900	19:00:00	313.361
21	08Aug2023 2000	20:00:00	302.556
22	08Aug2023 2100	21:00:00	291.75

Figure 15: Flow Hydrograph

2D Unsteady Flow Simulation

The hydraulic model was executed using the 2D unsteady flow solver in HEC-RAS 6.7. The simulation computed water surface elevation, flow depth, velocity distribution, and flood wave arrival time. The numerical engine solved the shallow water equations across the computational mesh, enabling realistic simulation of floodplain inundation processes.

3.3.3 Flood Inundation Mapping

Post-processing of simulation results was conducted in RAS Mapper to generate spatial flood products, including flood depth maps, water surface elevation grids, and flood extent polygons. The inundation boundary corresponding to the peak discharge condition was extracted to represent the maximum flood extent. These flood inundation maps were subsequently used for spatial impact assessment, comparison with satellite-derived flood extents (NDWI), and validation of ANN-driven hydraulic simulations.

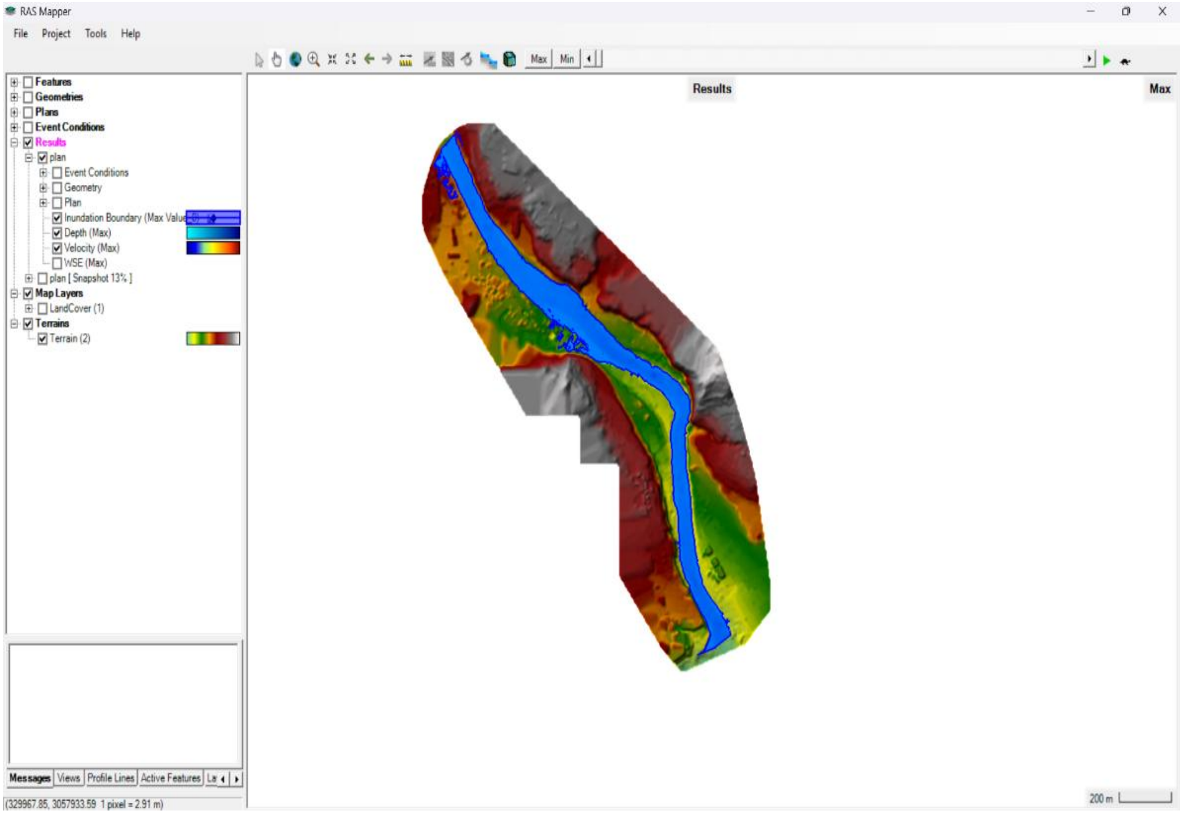

Figure 16: Inundation, velocity and Depth Result in HEC-RAS

3.3.4 Model calibration and validation

ANN model evaluation

The terms training and testing are commonly used instruments for checking of an accuracy and fitness of a model in hydrological modeling (Chuma et al., 2013; Desta & Lemma, 2017; Parhi, 2013) when ANN model is used as hydrological model. The performance of ANN hydrologic model result was trained with 4-years (2019-2022) climate data (rainfall, and temperature), with the target data (observed daily discharge) of the same periods (2019-2022) and also tested with 1 year (2022-2023) observed daily discharge. The performances in both periods (training and testing) were evaluated by Nash-Sutcliffe Efficiency (NSE).

Table 7: Model Fit Check parameters

S. N	Goodness of fit	NSE	PBIAS (%)	R^2
1	Very Good	$0.75 < NSE \leq 1$	$PBIAS < \pm10$	$R^2 > 0.85$
2	Good	$0.65 < NSE \leq 0.75$	$\pm10 < PBIAS \leq \pm15$	$0.75 < R^2 \leq 0.85$
3	Satisfactory	$0.5 < NSE \leq 0.65$	$\pm15 < PBIAS \leq \pm25$	$0.60 < R^2 \leq 0.75$
4	Unsatisfactory	$NSE \leq 0.5$	$PBIAS \geq \pm25$	$R^2 < 0.60$

However, Nash-Sutcliffe Efficiency (NSE) alone cannot give us the information on the model bias. The fitness of simulated versus observed evaluated in NSE should be supported by additional statistical error index model evaluation method. Therefore, the PBIAS as statistical error index model evaluation method was also used to check whether the model result was overpredicted or underpredicted and the equation for this model evaluation presented in Equation *2* (Ouali & Cannon, 2018; Pérez-Sánchez et al., 2019), and the corresponding criteria of fit for hydrological modeling for both model evaluation techniques.

Further, the ANN predictive hydrological model result was evaluated to describe the proportion of the variance between the observed and simulated values with the coefficient of determination, R^2. The general equation by which this coefficient is computed for the evaluation of a model is presented in Equation *5* (Pérez-Sánchez et al., 2019), and the acceptable range for hydrological modeling is given in the Table *7*.

$$R^2 = n * \left(\sum XY\right) - \left(\sum X\right) * \left(\sum Y\right) / [n \sum X^2 - \left(\sum X\right)^2] [n \sum Y^2 - \left(\sum X\right)^2$$

Equation 5: Coefficient of Determination (R^2)

Where, n = Number of data points

$\sum X$ = Sum of all X values

$\sum Y$ = Sum of all Y values

$\sum XY$ = Sum of the product of each pair ($X_i \cdot Y_i$)

$\sum X^2$ = Sum of squared X values

$\sum Y^2$ = Sum of squared Y values

HEC-RAS model evaluation

The runoff values obtained in ANN hydrological model was used as input in HEC-RAS to generate flood inundation areas. The inundation map generated in HEC-RAS during training (2019 - 2022) and testing (2023) periods were checked with the water body delineated using Normalized Difference Water Index (NDWI). The flood events of 2019,2023 were validated against the HEC-RAS model. NDWI uses Green (Band-3) and near infra-red (Band-5) bands of remote sensing images to extract a water body in which near-infrared (NIR) and short-wave infrared (SWI) are used as the main input. The NDWI raster was converted back to polygon by Raster to Polygon function. The performance evaluation between the inundation map generated in HEC-RAS and the water bodies delineated from remotely sensed LANDSAT 8 imagery in NDWI polygons were compared based on overlapping areas.

$$Overlapping\ Percentage\ (\%) = Layer_1(Km^2)/Layer_2(Km^2)$$

Equation 6: Overlapping Percentage

Where, $Layer_1$ is the area of the water body delineated in NDWI from flood events and $Layer_2$ is the area of the inundation map generated in HEC-RAS.

CHAPTER FOUR: RESULT AND DISCUSSION

4.1 ANN hydrological model result

The daily streamflow (runoff) values simulated by the ANN model for both training and testing periods are illustrated in Figure 17 & Figure 18. As shown in Figure 17, model performance during the four-year training period (2019 - 2022) demonstrated excellent agreement between simulated and observed discharges, with NSE = 0.95, PBIAS = 1.16%, and R^2 = 0.9622. For the one-year testing period (2023), presented in Figure 18, the model maintained good predictive capability, achieving NSE = 0.79, PBIAS = 13%, and R^2 = 0.80. Overall, the results confirm that the Artificial Neural Network model provides reliable and acceptable hydrological predictions, as summarized in Table 7.

Table 8: ANN Model Result

Period	**Years**	**NSE**	**R^2**	**PBIAS (%)**	Goodness of fit
Training	2019–2022	0.95	0.9622	1.16	Very Good
Testing	2023	0.79	0.80	13.00	Good

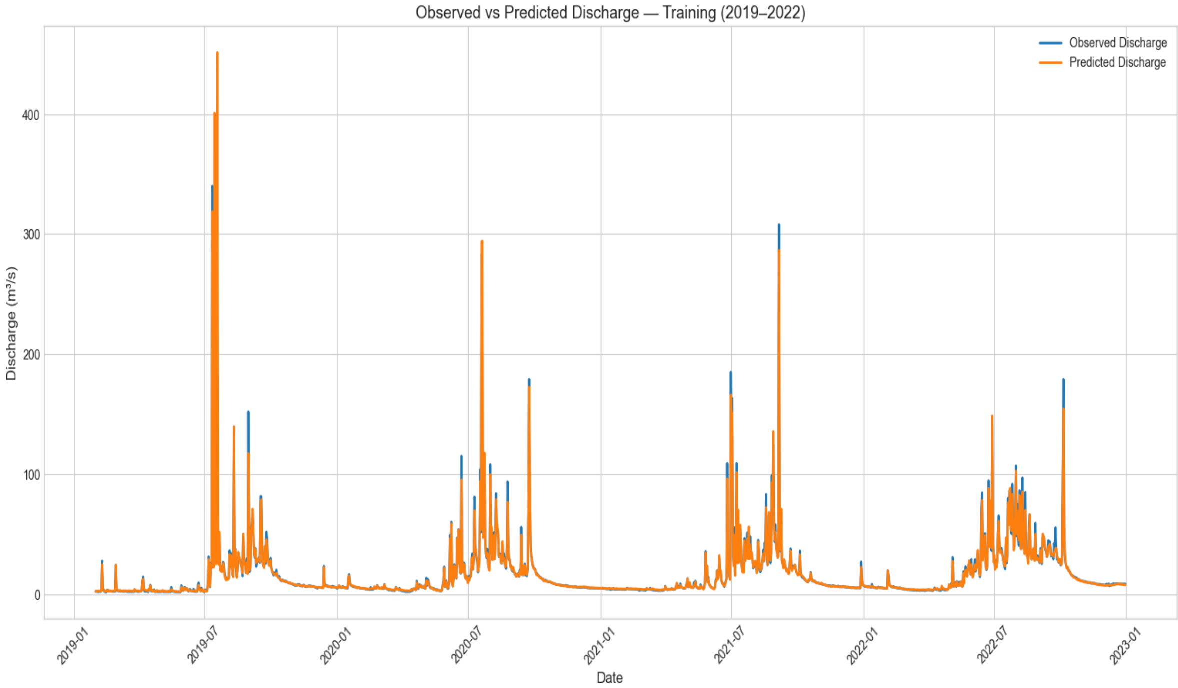

Figure 17: Training plot (2019-2022)

Figure 17 shows a time series plot comparing observed discharge values with those predicted by the ANN model during the training period from 2019 to 2022. The blue line represents the observed discharge, while the orange line represents the predicted discharge. Both lines are plotted against time, with the x-axis showing dates and the y-axis showing discharge in cubic meters per second (m^3/s). The plot contains several peaks and troughs, reflecting the natural variability of river discharge over time. By comparing the two lines, we can visually assess how closely the model predictions follow the actual measurements.

From the figure, it is clear that the predicted discharge closely tracks the observed discharge throughout the training period. The alignment of the two lines, especially during peak flow events, indicates that the ANN model has successfully learned the discharge patterns and can reproduce them with good accuracy. Although minor differences exist in some sections, the overall agreement between the observed and predicted values demonstrates strong model performance. This suggests that the ANN model is well-trained and capable of capturing both regular fluctuations and extreme events, making it a reliable tool for discharge forecasting and flood risk analysis.

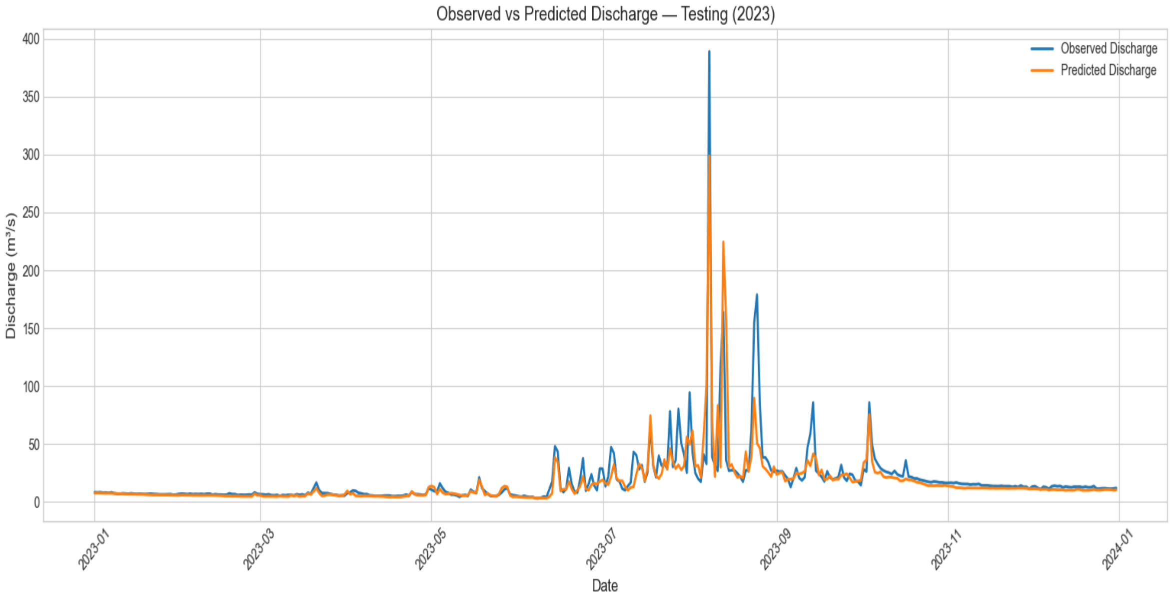

Figure 18: Testing plot (2023)

Figure 18 shows a time series plot comparing observed discharge values with those predicted by the ANN model during the testing period of 2023. The blue line represents the observed discharge, while the orange line represents the predicted discharge. Both lines are plotted against time, with the x-axis showing dates from early 2023 to early 2024 and the y-axis showing discharge in cubic meters per second (m^3/s). The plot captures the natural variability of river discharge, including several peaks and troughs, which reflect changes in rainfall and flow conditions. By comparing the two lines, we can visually assess how well the model predictions match the actual measurements.

From the figure, it is clear that the predicted discharge closely follows the observed discharge throughout most of the testing period. The alignment of the two lines demonstrates that the ANN model is able to reproduce discharge patterns with good accuracy. A significant peak is visible around mid-2023, where observed discharge rises above about 400 m^3/s. The predicted discharge also shows a sharp increase at the same time, though slightly lower than the observed value, indicating minor underestimation during extreme flow events. Despite these small differences, the overall agreement between the observed and predicted values highlights the model's strong performance and reliability. This suggests that the ANN model can effectively capture both regular fluctuations and peak flow conditions, making it a valuable tool for flood forecasting and risk management.

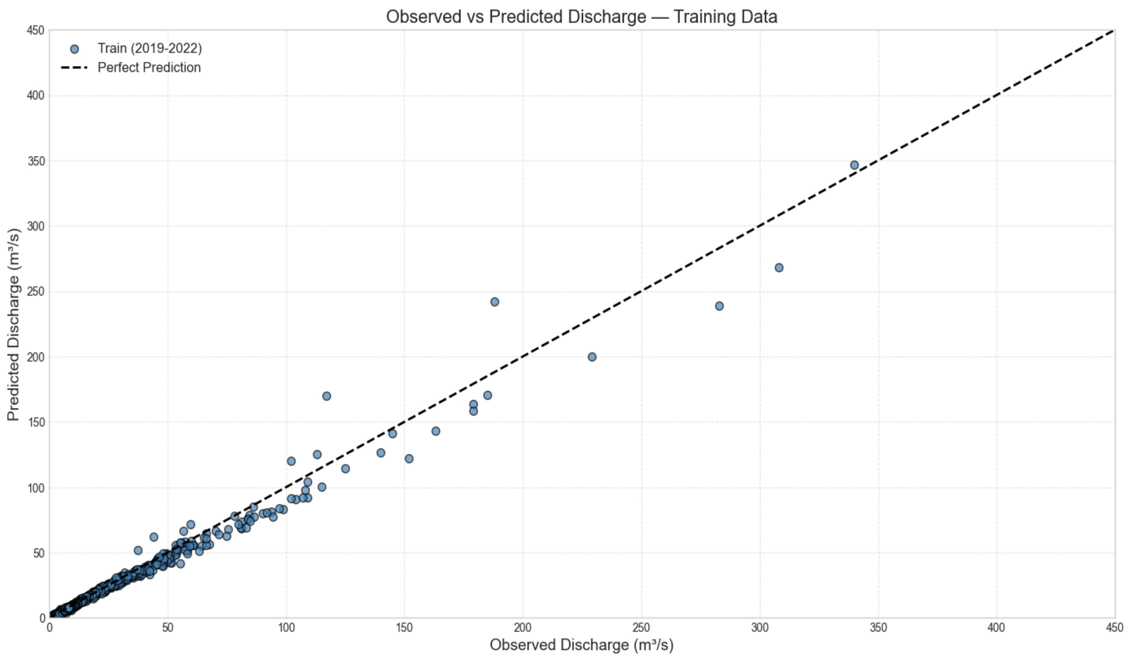

Figure 19: Scatter Plot between Observed and Predicted Discharge - Training Data

Figure 19 shows a scatter plot comparing observed discharge values with those predicted by the ANN model for the training dataset from 2019 to 2022. The observed discharge values are plotted on the x-axis, while the predicted values are shown on the y-axis. Each point represents one comparison between actual measurements and model predictions. A diagonal dashed line labeled “Perfect Prediction” is included, which indicates the condition where predicted values exactly match observed values. The closer the points are to this line, the better the model’s predictions align with reality.

From the figure, it is clear that most of the points lie close to the perfect prediction line, showing that the ANN model has learned the discharge patterns effectively during the training phase. This clustering near the line demonstrates a strong correlation between observed and predicted values, meaning the model is performing well. Although a few points deviate slightly, these differences are minor and expected in real-world data. Overall, the scatter plot highlights that the ANN model provides accurate and reliable predictions, making it a strong tool for discharge forecasting and flood risk analysis.

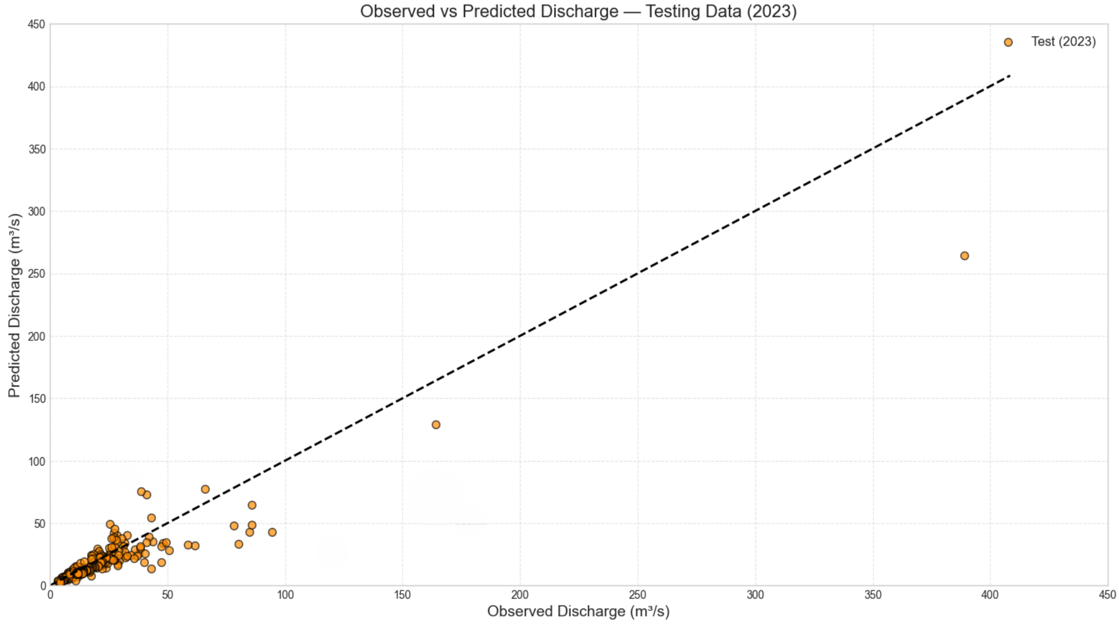

Figure 20: Scatter Plot between observed and predicted discharge - Testing Data (2023)

Figure 20 shows a scatter plot that compares the observed discharge values with the predicted discharge values from the ANN model for the testing dataset of 2023. The observed discharge values are plotted along the x-axis, while the predicted values are shown on the y-axis. Each brown dot represents one comparison between actual measurements and model predictions at a specific time. A diagonal dashed line is included to represent the "perfect match" condition, where predicted values would equal observed values. The closer the points are to this line, the better the agreement between the model's predictions and the real discharge measurements.

From the figure, it can be seen that most of the points are clustered near the diagonal line, which indicates that the ANN model is performing well and closely matches the observed discharge values. A few points, especially at higher discharge levels, deviate from the line, showing small errors in prediction during peak flow conditions. Despite these minor differences, the overall pattern demonstrates that the ANN model provides reliable predictions and captures discharge dynamics effectively. This makes the model a useful tool for flood forecasting and risk assessment in the Bagmati River basin.

4.2 HEC-RAS model output and validation

The HEC-RAS model was further evaluated using historical flood events on 2019 and 2023, corresponding to the calibration and validation periods. The inundation maps generated in HEC-RAS based on the ANN-simulated discharge for the years July 12th, 2019 and August 8th, 2023 were compared with the water bodies delineated using the Normalized Difference Water Index (NDWI) for the same flood events. The results are presented in figure respectively.

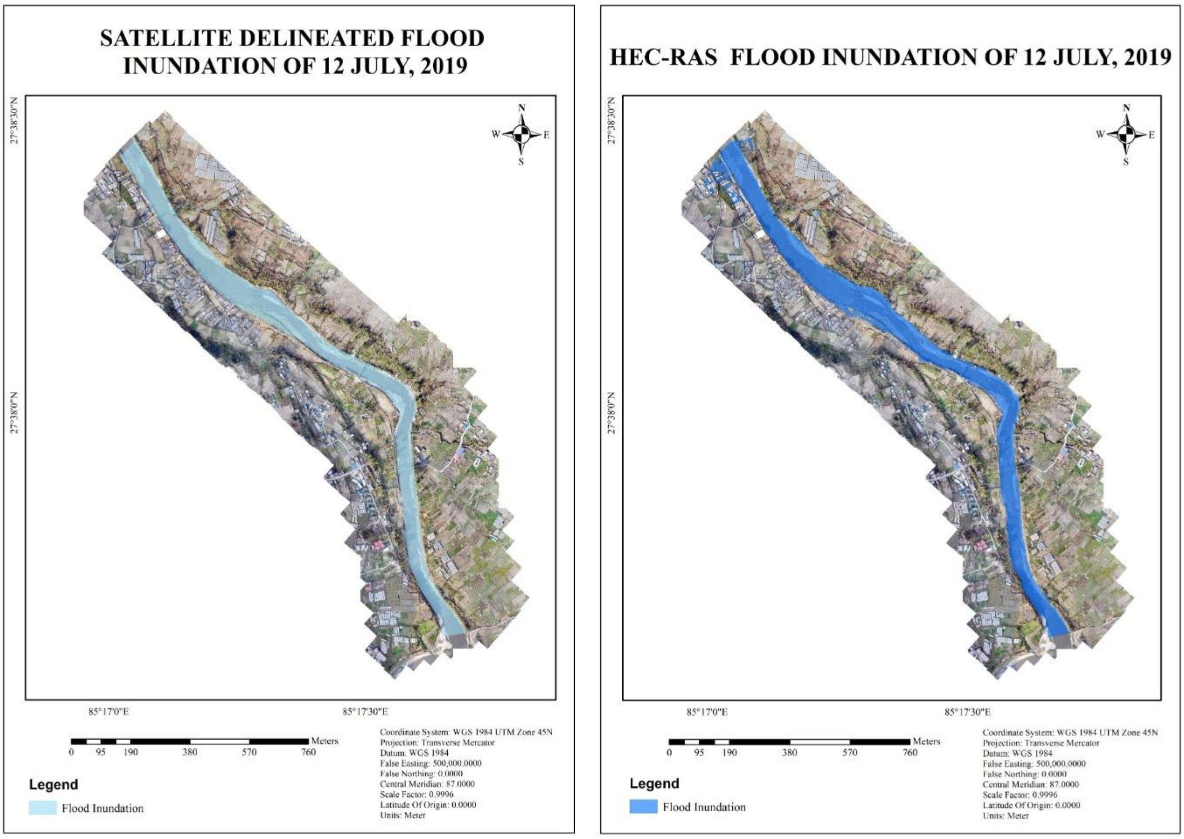

Figure 21: Satellite & HEC-RAS result for Flood Inundation 12 July, 2019 respectively.

From the overlapping percentage areas computed in ArcGIS pro, 88 % of intersected areas were counted from the inundation map generated in HEC-RAS and water body delineated in NDWI during the calibration and validation periods for year 2019.

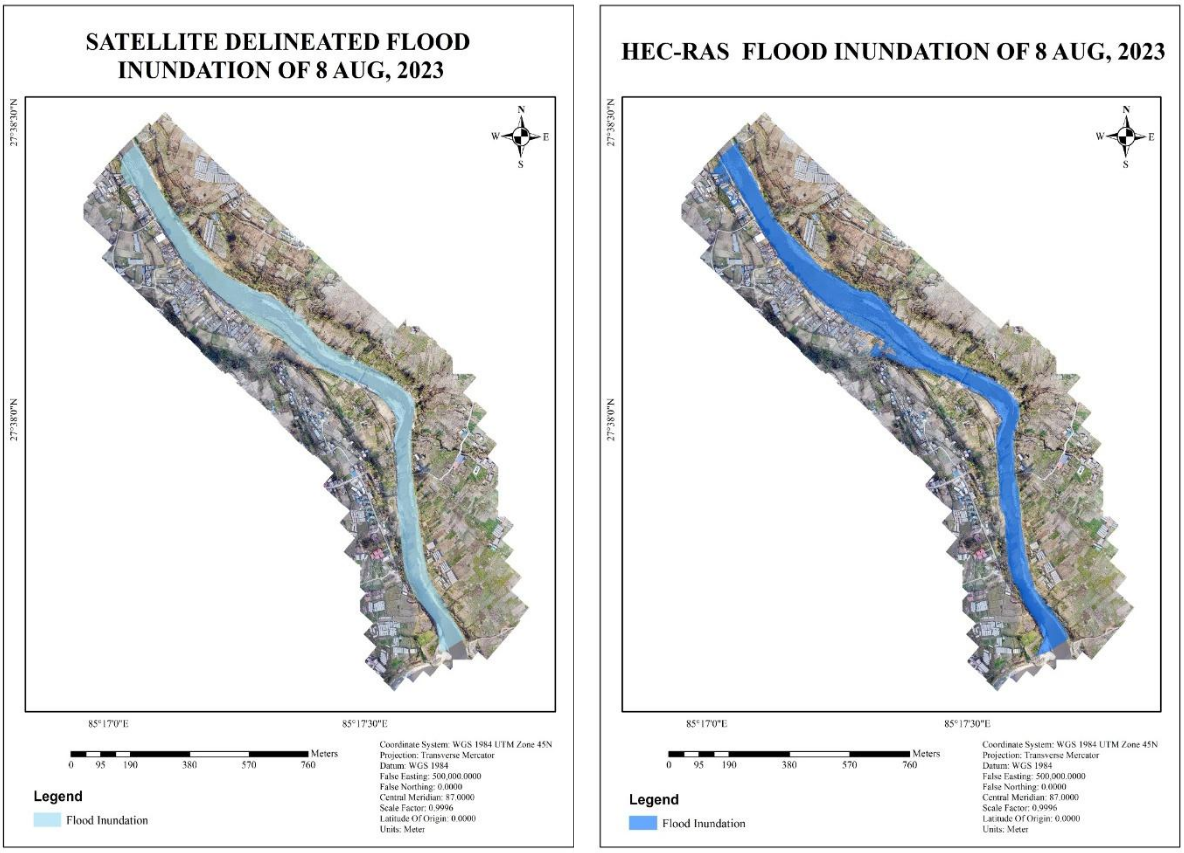

Figure 22: Satellite & HEC-RAS result for Flood Inundation 8 Aug, 2023 respectively.

Similarly, From the overlapping percentage areas computed in ArcGIS pro,86 % of intersected areas were counted from the inundation map generated in HEC-RAS and water body delineated in NDWI during the calibration and validation periods for year 2023.

According to the studies conducted by (Bagherzadeh & Daneshvar, 2011; Mai & De Smedt, 2017), the inundation map was evaluated based on the overlapping areas and if more than 85 % counted percentage of overlapped, it is considered as a good agreement. The ability of an integrated data-driven approach and HEC-RAS model in improving the accuracy of prediction and generation of flood inundation is clearly seen in this study.

4.3 Limitation

- The ANN discharge model relied on rainfall, temperature, and discharge records obtained from available stations. Sparse spatial distribution of stations may not fully capture localized rainfall variability across the watershed, which can reduce discharge prediction accuracy particularly during extreme storm events.
- Flood validation using NDWI depends on satellite overpass timing. Any temporal mismatch between peak flood occurrence and image acquisition can lead to Underestimation if water receded before capture.

4.4 Recommendations

Based on the outcomes of this study, several recommendations are proposed to improve the accuracy, reliability, and practical application of flood discharge prediction and inundation mapping. These recommendations aim to guide future research, enhance disaster preparedness, and support sustainable land-use planning in flood-prone regions.

- Incorporate soil moisture, infiltration capacity data to improve rainfall–runoff modeling.
- Use extended historical discharge and meteorological records to strengthen model robustness and predict extreme events.
- Integrate model outputs into real-time flood forecasting and community-based early warning systems.

4.5 Comparative Analysis with Reference Paper

The comparative results between the Nepal and Ethiopia studies highlight how the ANN–HEC-RAS framework adapts to different hydrological and geographical contexts. In Nepal's Bagmati–Khokana project, the ANN model achieved very high accuracy during training, with an NSE of 0.95, R^2 of 0.9622, and a PBIAS of just 1.16%, all classified as "Very Good." When tested against independent 2023 data, performance dropped slightly to an NSE of 0.79, R^2 of 0.80, and PBIAS of 13%, which is still considered "Good." Importantly, the final spatial validation showed an overlap of 86–88% between simulated flood extents and NDWI-derived footprints, confirming strong agreement. This reflects the challenges of generalizing predictions in the flashy and complex hydrology of the Bagmati River, where rapid urbanization and micro-topographic variations strongly influence flood behavior. The strength of the Nepal study lies in its use of ultra-high-resolution UAV-derived terrain data (14.9 cm), which allowed precise representation of embankments and floodplain features, making the inundation maps particularly valuable for urban flood risk management and cultural heritage protection in Khokana.

By contrast, the Ethiopian Baro Akobo Basin study demonstrated consistently strong performance across both training and testing phases. The ANN model achieved NSE values of 0.86–0.88, R^2 between 0.91–0.93, and PBIAS around 8%, all within the "Very Good" category. Importantly, spatial validation showed excellent agreement, with 94.6% overlap during calibration and 96% during validation between simulated inundation and NDWI-derived flood footprints. Although the study relied on 30 m DEM data, it proved robust at a basin-wide scale, successfully capturing flood depths up to 250 cm and providing reliable hazard mapping for regional flood management(Tamiru & Wagari, 2022b).

In summary, Nepal's model excels in localized precision due to ultra-high-resolution terrain integration but shows moderate variability in testing, while Ethiopia's model demonstrates consistent reliability across broader spatial and temporal scales. Together, they illustrate how ANN–HEC-RAS integration can be tailored: Nepal emphasizes fine-scale urban resilience, whereas Ethiopia highlights basin-scale robustness.

CHAPTER FIVE: CONCLUSION

This study successfully demonstrates the effectiveness of an integrated Machine Learning–hydraulic modeling framework in producing high-precision flood inundation maps within the data-scarce and rapidly urbanizing environment of the Bagmati River Basin at Khokana, Nepal. By coupling Artificial Neural Network (ANN)–based discharge prediction with two-dimensional hydraulic simulation in HEC-RAS the research achieved exceptional model performance, evidenced by a Nash-Sutcliffe Efficiency (NSE) of 0.95 and R^2 of 0.96 during training (2019-2022), and NSE of 0.79 with R^2 of 0.80 during testing (2023). Validation against satellite-derived Normalized Difference Water Index (NDWI) data for historical flood events in 2019 and 2023 revealed strong spatial agreement, with overlapping inundation areas 86–88%, surpassing benchmarks for "good agreement" in similar studies. The incorporation of high-resolution Digital Terrain Models (DTM) generated via UAV photogrammetry and DGPS surveys - achieving centimeter - level accuracy - proved transformative, capturing intricate floodplain topography and features those traditional low-resolution datasets (e.g., SRTM or ASTER) often overlook.

This hybrid ANN-HEC-RAS approach addresses critical gaps in conventional flood modeling, particularly in regions like Nepal where hydro-meteorological data is sparse and urban encroachment exacerbates flood risks. The integration of machine learning–based discharge forecasting with physically based hydraulic modeling proved particularly valuable in data-scarce environments.

Overall, the project provides a robust, scalable, and replicable approach for flood inundation modeling, particularly suitable for rapidly urbanizing and flood-prone regions. The outcomes of this research can support disaster risk reduction planning, infrastructure protection, and community-level flood preparedness.

REFERENCES

Abhishek, K., Kumar, A., Ranjan, R., & Kumar, S. (2012). A data-driven model for rainfall-runoff forecasting using artificial neural networks. *International Journal of Computer Science Issues*, *9*(3), 582.

Adhikari, A., & Sharma, S. (2018). Flood hazard mapping of the Bagmati River, Nepal, using HEC-RAS and GIS. *Journal of Hydrological Sciences*, *63*(11), 1589–1602.

Bagherzadeh, A., & Daneshvar, M. R. M. (2011). Physical land suitability evaluation for specific cereal crops using GIS at Mashhad Plain, Northeast of Iran. *Frontiers of Agriculture in China*, *5*(4), 504–513. https://doi.org/10.1007/s11703-011-1102-6

Bhattacharya, N., Misra, R. K., & Das, S. (2020). Impact of Digital Elevation Model (DEM) resolution on flood inundation modeling in complex urban landscapes. *International Journal of Geoinformatics*, *16*(2), 45–58.

Centre for Research on the Epidemiology of Disasters. (2024). *2023 disasters in numbers*. UCLouvain. https://www.cred.be

Chuma, C., Orimoogunje, O. O. I., Hlatywayo, D. J., & Akinyede, J. O. (2013). Application of remote sensing and geographical information systems in determining the groundwater potential in the crystalline basement of Bulawayo metropolitan area, Zimbabwe. *Advances in Remote Sensing*, *2*(2), 149–161. https://doi.org/10.4236/ars.2013.22019

Desta, H., & Lemma, B. (2017). SWAT based hydrological assessment and characterization of Lake Ziway sub-watersheds, Ethiopia. *Journal of Hydrology: Regional Studies*, *13*, 122–137. https://doi.org/10.1016/j.ejrh.2017.08.002

Gautam, D. K., & Kharbuja, M. L. (2006). Flood management in Nepal. *Proceedings of the International Workshop on Flash Flood Management and Sustainable Development in the Himalayas*.

Horstmann, A., & Wenzel, K. (2019). UAV-based photogrammetry for high-fidelity DEM generation in local-scale hydraulic studies. *Proceedings of the International Conference on Geomatics and Flood Management*.

Mai, D. T., & De Smedt, F. (2017). A combined hydrological and hydraulic model for flood prediction in Vietnam applied to the Huong river basin as a test case study. *Water*, *9*(11). https://doi.org/10.3390/w9110879

Mosavi, A., Ozturk, P., & Chau, K. W. (2018). Flood prediction using machine learning models: Literature review. *Water*, *10*(11), 1536. https://doi.org/10.3390/w10111536

Ouali, D., & Cannon, A. J. (2018). Estimation of rainfall intensity–duration–frequency curves at ungauged locations using quantile regression methods. *Stochastic Environmental Research and Risk Assessment*, *32*(10), 2821–2836. https://doi.org/10.1007/s00477-018-1564-7

Pandey, B. K., Kumar, R., & Devkota, L. P. (2020). Inundation mapping and hazard assessment of the Bagmati River Basin using HEC-RAS. *Nepal Journal of Science and Technology*, *21*(1), 88–97.

Parhi, P. K. (2013). HEC-RAS model for manning's roughness: A case study. *Open Journal of Modern Hydrology*, *3*(3), 97–101. https://doi.org/10.4236/ojmh.2013.33013

Pérez-Sánchez, J., Senent-Aparicio, J., Segura-Méndez, F., Pulido-Velazquez, D., & Srinivasan, R. (2019). Evaluating hydrological models for deriving water resources in peninsular Spain. *Sustainability*, *11*(10), 1–36. https://doi.org/10.3390/su11102872

Sampson, C. C., Smith, A. M., Bates, P. D., Neal, J. C., Alfieri, L., & Freer, J. E. (2015). A high-resolution global flood hazard model. *Water Resources Research*, *51*(9), 7358–7381. https://doi.org/10.1002/2015WR016954

Sharma, V., & Gupta, R. (2021). Hybrid modeling in hydrology: Integrating machine learning and physical models for flood forecasting. *Journal of Hydroinformatics*, *23*(4), 712–729.

Shrestha, M. S. (2019). Flood Frequency Analysis and risk assessment of the Bagmati River, Nepal. *Journal of Flood Risk Management*, *12*(S1), e12456.

Tamiru, H., & Wagari, M. (2022a). Flood inundation mapping and hazard assessment under climate change scenarios using HEC-RAS and GIS. *Natural Hazards*, *114*, 2183–2202. https://doi.org/10.1007/s11069-022-05451-9

Tamiru, H., & Wagari, M. (2022b). Flood inundation mapping using integrated HEC-RAS and Artificial Neural Network: A case study of Baro River Basin, Ethiopia. *Applied Water Science*, *12*(10), 234. https://doi.org/10.1007/s13201-022-01750-z

Thapa, S., Talchabhadel, R., Kanel, J., & Iseri, Y. (2020). Impact of land use and land cover change on discharge and sediment yield of the Bagmati River Basin, Nepal. *Journal of Hydrology: Regional Studies*, *30*. https://doi.org/10.1016/j.ejrh.2020.100709

UNESCO. (2023). *The United Nations world water development report 2023: Partnerships and cooperation for water*. UNESCO.

United States Army Corps of Engineers. (2020). *HEC-RAS, river analysis system hydraulic reference manual, Version 6.0*. Hydrologic Engineering Center.

Wedajo, G. K., Ayana, M., & Megersa, O. (2024). Data-driven feature selection for flood causative factors: A case study of the Awash River Basin, Ethiopia. *Environmental Earth Sciences*, *83*(2), 115–130.

APPENDICES

APPENDIX-1: Field Reconnaissance: Bagmati River - Khokana, Lalitpur



APPENDIX-2: Drone Flight Permission from District Administration Office

फोन ९०१-५५२११६५/५५५२८५५
ईमेल: daolalitpur5@gmail.com
वेबसाइट: www.daolalitpur.moha.gov.np

नेपाल सरकार
गृह मन्त्रालय
जिल्ला प्रशासन कार्यालय
स्थानीय प्रशासन शाखा

मानभवन, ललितपुर
बागमती प्रदेश
मिति:२०८२।०९।०७
नेपाल सम्वत्:११४६, पोहेलाथ्व द्वितीया

पत्र संख्या: २०८२/२०८३
चलानी नम्बर: ४२१६

नेपाल सरकार
गृह मन्त्रालय
जिल्ला प्रशासन कार्यालय
ललितपुर

श्री काठमाडौं विश्वविद्यालय
स्कुल अफ इन्जिनियरिङ, धुलिखेल काभ्रे।

विषय: ड्रोन उडान अनुमति सम्बन्धमा।

प्रस्तुत विषयमा काठमाडौ विश्वविद्यालय स्कुल अफ इन्जिनियरिङ धुलिखेल काभ्रेको मिति २०८२।०९।०२ गतेको प्राप्त पत्रबाट माग भई आएअनुसार हवाई उपकरण उडान सम्बन्धी कार्यविधि २०७५ को नियम पालना गर्ने गरी बढीमा २ के.जी. सम्मको ड्रोन उडानका लागि ललितपुर महानगरपालिका वडा नं.१८, २१ र २२ का निषेधित क्षेत्र बाहेकका स्थानहरुमा मिति २०८२।०९।०६ गतेदेखि ऐ.१३ गतेसम्म ड्रोन उडानका लागि स्वीकृती दिइएको व्यहोरा आदेशानुसार अनुरोध छ।

२०८२।०९।०७

ज्योत्स्ना भट्ट जोशी
प्रशासकीय अधिकृत

प्रशासकीय अधिकृत

बोधार्थ:
श्री जिल्ला प्रहरी परिसर
जावलाखेल, ललितपुर।

व्यावसायिक र सिर्जनशील प्रशासन, विकास, समृद्धि र सुशासन

APPENDIX-3: DGPS Survey for Control Point Establishment

APPENDIX-3: UAV Survey at Bagmati River – Khokana, Nepal

APPENDIX-4: ANN Model Code

newannfchat.py 9+ X

C: > Users > legion > AppData > Local > Packages > 5319275A.WhatsAppDesktop_cv1g1gvanyjgı

```python
# =========================================================
# DISCHARGE PREDICTION ANN
# Train: 2019–2022 | Test: 2023
# =========================================================

import pandas as pd
import numpy as np
import torch
import torch.nn as nn
from torch.utils.data import Dataset, DataLoader
from sklearn.preprocessing import StandardScaler
from sklearn.metrics import mean_squared_error, r2_score
import joblib
import matplotlib.pyplot as plt

# ==============================
# 1. LOAD DATA
# ==============================

data_path = r"D:\FInal Year\hackfest\finalyear\merged_final.csv"

df = pd.read_csv(data_path)

df['Date'] = pd.to_datetime(df['Date'])
df = df.sort_values('Date').reset_index(drop=True)
df = df.ffill().bfill()

# ==============================
# 2. FEATURE ENGINEERING
# ==============================

lags = [1,2,3,4,7,10,14,21,30]

for lag in lags:
    df[f'lag{lag}'] = df['Discharge'].shift(lag)

# Rain features
df['rain_3'] = df['Average_Rainfall_mm'].rolling(3).mean()
df['rain_7'] = df['Average_Rainfall_mm'].rolling(7).mean()
df['rain_14sum'] = df['Average_Rainfall_mm'].rolling(14).sum()
df['rain_30sum'] = df['Average_Rainfall_mm'].rolling(30).sum()
df['rain_3max'] = df['Average_Rainfall_mm'].rolling(3).max()
df['rain_ema3'] = df['Average_Rainfall_mm'].ewm(span=3).mean()
df['rain_ema7'] = df['Average_Rainfall_mm'].ewm(span=7).mean()

# API
df['rain_lag1'] = df['Average_Rainfall_mm'].shift(1)
df['rain_lag2'] = df['Average_Rainfall_mm'].shift(2)
df['rain_lag3'] = df['Average_Rainfall_mm'].shift(3)

df['API'] = (0.85*df['rain_lag1'] +
             0.72*df['rain_lag2'] +
             0.61*df['rain_lag3'])

# ==============================
# 3. FEATURES
# ==============================

features = [
    'Average_Rainfall_mm','average_min_temp','Average_max_temp',
    *[f'lag{i}' for i in lags],
    'rain_3','rain_7','rain_14sum','rain_30sum','rain_3max',
    'rain_ema3','rain_ema7','API',
    'flow_7mean','flow_14mean',
    'temp_range','sin_doy','cos_doy'
]

target = 'Discharge'

# ==============================
# 4. SPLIT DATA
# ==============================

train_df = df[(df['Date'].dt.year >= 2019) &
              (df['Date'].dt.year <= 2022)]

test_df  = df[df['Date'].dt.year == 2023]

X_train = train_df[features].values
y_train = train_df[target].values.reshape(-1,1)

X_test  = test_df[features].values
y_test  = test_df[target].values.reshape(-1,1)

# ==============================
# 5. LOG TRANSFORM
# ==============================

OFFSET = 1e-6

y_train_log = np.log1p(y_train + OFFSET)
y_test_log  = np.log1p(y_test + OFFSET)

# ==============================
# 6. SCALING
# ==============================

scaler_X = StandardScaler()
scaler_y = StandardScaler()

X_train_scaled = scaler_X.fit_transform(X_train)
X_test_scaled  = scaler_X.transform(X_test)

y_train_scaled = scaler_y.fit_transform(y_train_log)
y_test_scaled  = scaler_y.transform(y_test_log)
```

```python
# ==============================
# 8. ANN MODEL
# ==============================

class ANNModel(nn.Module):
    def __init__(self,input_size):
        super().__init__()

        self.net = nn.Sequential(
            nn.Linear(input_size,256),
            nn.ReLU(),
            nn.BatchNorm1d(256),
            nn.Dropout(0.2),

            nn.Linear(256,128),
            nn.ReLU(),
            nn.BatchNorm1d(128),
            nn.Dropout(0.15),

            nn.Linear(128,64),
            nn.ReLU(),

            nn.Linear(64,1)
        )

    def forward(self,x):
        return self.net(x)

device = torch.device(
    "cuda" if torch.cuda.is_available() else "cpu")

model = ANNModel(len(features)).to(device)

# ==============================
# 9. PEAK WEIGHTED LOSS
# ==============================

def peak_weighted_loss(pred,target):
    weight = 1 + 2*(target > target.mean())
    return torch.mean(weight*(pred-target)**2)

optimizer = torch.optim.Adam(
    model.parameters(),lr=0.001)

scheduler = torch.optim.lr_scheduler.ReduceLROnPlateau(
```

```python
# ============================================================
# ANN DISCHARGE PREDICTION — PAST + FUTURE
# Copy-Paste Ready for VS Code
# ============================================================

import pandas as pd
import numpy as np
import torch
import torch.nn as nn
import joblib
from datetime import timedelta

# ==============================
# FILE PATHS (EDIT IF NEEDED)
# ==============================

data_path    = r"D:\FInal Year\hackfest\finalyear\merged_final.csv
model_path   = "discharge_ann_model1.pth"
scalerX_path = "scaler_X.pkl"
scalery_path = "scaler_y.pkl"

# ==============================
# LOAD DATA
# ==============================

df_base = pd.read_csv(data_path)
df_base['Date'] = pd.to_datetime(df_base['Date'])
df_base = df_base.sort_values('Date').reset_index(drop=True)
df_base = df_base.ffill().bfill()

# ==============================
# LOAD SCALERS
# ==============================

scaler_X = joblib.load(scalerX_path)
scaler_y = joblib.load(scalery_path)

# ==============================
# FEATURES
# ==============================

lags = [1,2,3,4,7,10,14,21,30]

FEATURES = [
    'Average_Rainfall_mm','average_min_temp','Average_max_temp',
    *[f'lag{i}' for i in lags],
    'rain_3','rain_7','rain_14sum','rain_30sum','rain_3max',
    'rain_ema3','rain_ema7','API',
    'flow_7mean','flow_14mean',
    'temp_range','sin_doy','cos_doy'
]
```

APPENDIX-5: DEPTH MAP(MAX) of 2018 & 2023

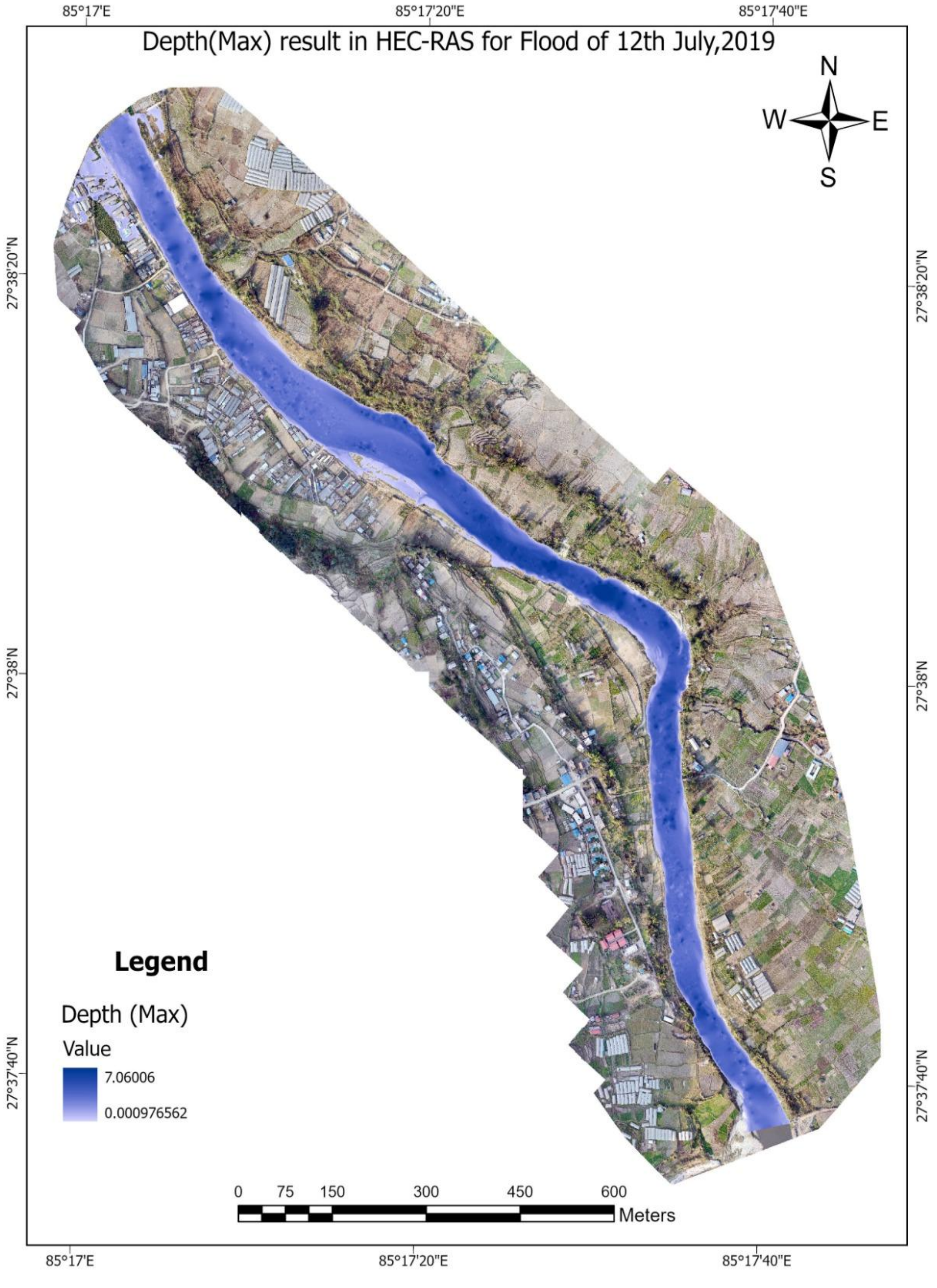

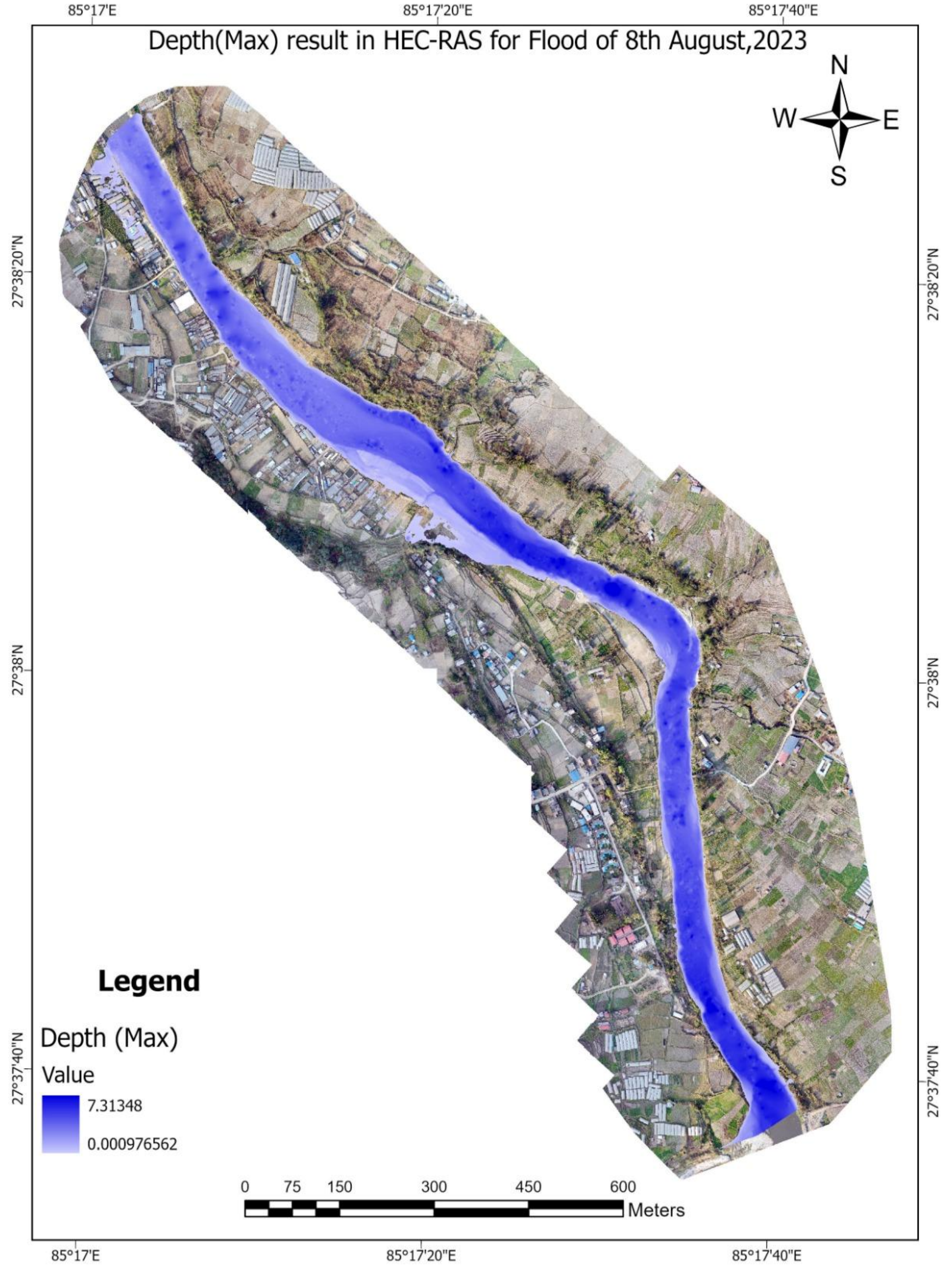

85°17'E
85°17'20"E
85°17'40"E
Depth(Max) result in HEC-RAS for Flood of 8th August,2023
N
W
E
S
27°38'20"N
27°38'N
27°37'40"N
Legend
Depth (Max)
Value
7.31348
0.000976562
0 75 150 300 450 600
Meters